

## **Authors' response to comments on "ATAT 1.0, an Automated Timing Accordance Tool for comparing ice-sheet model output with geochronological data"**

*Responses in italics.*

*We thank both reviewers for their comments which have helped focus and clarify the manuscript. We have made changes to both the manuscript and the code having considered these comments. On the code, we have incorporated aspects of model uncertainty (margin position, elevation) into the code, and programmed the code in such a way that it can be called from the command-line and is therefore more suitable for batch processing (e.g. of a large ensemble). Changes were substantial enough that we now call this version of the code 1.1.*

*Line numbers below refer to the document which includes track changes.*

### **Reviewer 1: Evan Gowan**

#### **General comment**

Ely et al. present a tool that can be used to evaluate an ice sheet reconstruction or the output of an ice sheet model simulation to chronological data relating to the minimum timing of retreat or maximum timing of advance. I think such a tool is very valuable, and I can see it being useful in my own studies. As stated in the paper, there have been few attempts to directly incorporate individual dates into ice sheet reconstruction evaluation, instead using margin reconstructions such as those by Dyke (2004) and Hughes et al. (2016) for visual comparison. Ely et al. use a statistical approach to evaluate whether or not the area covered by the ice sheet reconstruction is consistent with the chronological information that indicates ice free conditions. As stated in the manuscript, all dates suffer from the "minimum age problem", which is to say that there is an unknown period of time between the retreat of the ice sheet and the age of the material dated (although cosmogenic dates might be close). However, there are few other options to directly evaluate how close the reconstruction is to reality. ATAT is a valuable addition for assessing ice sheet reconstructions that should be used alongside other evaluation methods such as fit to glacial isotopic adjustment indicators.

*We are glad that the reviewer sees the value in our tool. On their final point, we have now made it explicit in the text that ATAT should be used in conjunction with other evaluation methods, including GIA (lines 47-48 and 553-554).*

#### **1. ATAT software**

Unfortunately, I was unable to get the software to work. I tried to follow the instructions for the format of the NetCDF file as per Table 3, but the program would not accept them, specifically with the geochronological data file. I would suggest adding scripts to build this file, or at least give some example NetCDF files so that it is possible to put things in the right format.

*We now have an example NetCDF file in the supplementary material for guidance on how to build the geochronological file.*

It should be noted that the unit "Years before present" is not a valid CF compliant time unit, and will cause command line NetCDF tools like CDO to complain and not work. I would use CF compliant units to make the NetCDF files compatible with other programs.

*The provided example netcdf now uses valid CF compliant units, with a calendar the same as that of the ice-sheet model (in our case years before 1-1-1). We have addressed the calendar issue in the text (Lines 366-367).*

There is no recommendation on what to do if there are multiple dates in one grid cell. When I was attempting to use the program, I just took the oldest date without regard of the error, but maybe it is better to make a combined probability using a tool like OxCal (Bronk Ramsey, 2009).

*The selection of dates for each cell should be left to expert judgement. The issue of data quality is paramount when choosing a geochronological constraint and requires expert judgement – as explored in Small et al. (2017). We have made it more explicit that such expert judgement is needed for individual cells (lines 369-372), and that future attempts should incorporate Bayesian modelling (as per Chiverrell et al., 2013, lines 379-382). In reality, with a high-resolution ice-sheet model (say 5 km) it is unlikely that two equally reliable dates will be contained within a cell – radiocarbon in a core for example should just use the date that is oldest, closest to the glacial contact.*

Are the errors supposed to be 1-sigma or 2-sigma? The paper does not indicate which should be used.

*This is up to the user, and will vary for experimental design. 1 or 2 sigma could also depend upon the source of data for a cell – radiocarbon is typically reported as 2 sigma, OSL as 1. We have reported this in the text (372-375).*

Also, calibrated radiocarbon dates are not normally distributed, what is the recommendation for usage in this program?

*We are using minimum (maximum) constraints for deglaciation (advance), we only look at one side of the distribution (one-tailed constraints as in our Fig. 3). We therefore have an agree/disagree metric that is not dependent upon distribution shape, but rather a user defined acceptable level of error. This is now mentioned in the text (373-375).*

Another recommendation I would have is to allow the program to read the required variables (i.e. DEGLACIAL/ADVANCE, filenames, THK/MASK) from a file rather than requiring interactive input. This would greatly streamline usage in scripts where many ice sheet reconstructions are evaluated and plotted automatically.

*We now enable users to specify all options at the command line, rather than interactively. Scripts could then be developed to batch process several files. The text has been changed throughout to accommodate this change.*

## 2. Paper

In general, the paper is well written, though I think at times the authors go overboard on detail that is not directly relevant to the tool they are introducing. I think section 2 (background) should be shortened considerably. In the current form, it is almost half of the text. In particular, section 2.2 is a two and a half page review of the inadequacies of ice sheet

models. I don't think Geoscience Model Development is really an appropriate venue for such a review, especially since ATAT is not really about fixing these problems. Bringing up these issues here really gives the impression that the authors don't trust ice sheet models at all, which I doubt is the intention. I think anyone doing ice sheet modeling is well aware that it may not be possible to exactly reproduce a configuration that replicates geological observations given the limitations of the models, but they may want to know how close they are!

*Though we have reduced the length of this section, we think it is important to review these inadequacies of ice sheet models here. We note that whenever ice-sheet models are demonstrated to non-modellers interested in palaeo-ice sheets, they often question why a specific site or geologically recorded event is not accurately replicated. Though people who conduct ice-sheet modelling are aware of the limitations of models, those in the palaeo-community who do not conduct ice sheet model experiments (half the audience for this paper) are often unaware of model limitations. We note that we also have a lengthy review of the inadequacies of dating, useful for modellers who may not be so close to this discipline. We also disagree that ATAT, and tools like this, won't fix model these problems. Albeit in an indirect way, such comparisons can help. This rationale was stated in the manuscript (299-307), and has been reiterated in the introduction (lines 79-84).*

I think rather than going into such detail on the inadequacies of ice sheet models, it would be more appropriate to detail how ice sheet reconstructions are numerically evaluated at present, such as the extensive Monte Carlo sampling technique used by Lev Tarasov (e.g. Tarasov et al., 2012) and evaluations based purely on glacial isostatic adjustment (e.g. Auriac et al., 2016).

*We mention the use of GIA modelling in the introduction and have added the Auriac reference (line 59). Tarasov et al. 2012 run ice sheet models that are not independent of the dated chronology (there is a margin raster, their Fig 2, which "nudges" the ice sheet into place based upon Dykes reconstruction). This calibration is different to model evaluation. We have reduced the uncertainty section, but note that without pointing out the inadequacies of ice-sheet models, we think it would be difficult to make a valid comparison.*

Section 3 does a nice job of explaining the usage of ATAT.

In section 4 and 5, there is a lot of emphasis that this tool be used with large ensemble of model runs. I don't know if this is a realistic outlook if you want to consider realistic climate scenarios. Computing a specific climate state (e.g. LGM) can take weeks, and a fully coupled ice sheet-climate model is along the lines of months. While ice sheet modelling by itself takes a lot less time to run, I question how valid it is to run a large ensemble of model runs using a linear scaling of modern day climate. During glacial periods, the ocean and atmospheric patterns were substantially perturbed, and this has follow-on impacts on the growth and retreat of ice sheets. Maybe such an exercise is useful to get a general feel for the kind of climatic conditions are necessary for glaciation, but I don't think it is diagnostic. The discrepancies between the three model runs presented in this section and the chronological data could very well be due to this issue. It could also be related to using a scaling based on the GRIP record, which may not be representative of the climatic variability in the British Isles during the Weichselian Glaciation. None of these points detract from the utility of ATAT, and I think the focus should be more on evaluating the model results. Perhaps one way to do

this is to run ATAT using the DATED reconstruction and compare it with one of the model runs. This would illustrate what a good fit looks like.

*We agree that perturbing modern climate by a distal climate record will not capture all of the necessary climate changes. However, this is still done by some palaeo-ice sheet modellers (e.g. Patton et al. 2016 and 2017, Seguinot et al. 2016) to reconstruct these ice masses. ATAT could be used to decipher how well these models simulate the glacial history of an area.*

*However, coupled earth-system models are also being developed which will capture oceanic and atmosphere changes. It will be important to evaluate how close to the data these runs achieve, and where improvement is needed.*

*We have now made it explicit that these 3 model runs are for demonstration purposes only, and our intention is to highlight the utility of ATAT, not to accurately capture climatic conditions over Britain and Ireland through the last deglacial (lines 492-494).*

### 3. Minor comments

Line 57: I would include Auriac et al. (2016) here.

*Auriac et al (2016) now included.*

Line 301: The sentence here is not complete.

*Now fixed.*

Line 441: Any reason for using the SPECMAP sea level curve rather than more up to date reconstructions?

*No. We just had SPECMAP available. As noted, the aim of these simulations are just to provide a bank of 3 simple experiments to compare to geochronological data.*

Figure 7: There is no frame of reference in these maps. I'd suggest putting on modern shorelines to make it easier to see what is going on with the model output.

*Coastlines have been added to this figure.*

Figure 8: It is very hard to see the location of the geochronological data on these plots. Maybe it would be better to just plot the raw data as points, rather than plotting them as a grid. I also find it a bit confusing to put both the timing of advance to the maximum extent and the Younger Dryas readvances on the same plot. I suggest splitting it up into two panes.

*We have plotted the data as points rather than cells for visual clarity. The younger dryas is included to highlight that ATAT only includes the last advance of ice (model could be stopped before younger dryas for a different experiment).*

### **Reviewer 2: Lev Tarasov**

After a long description of data and model uncertainties, the authors present a description and example application of a data-model comparison software tool. As detailed below, I find several flaws in the proposed data-model comparison algorithm that need to be addressed. Furthermore, I do not understand why the authors place so much attention on model uncertainty in the text and then fully ignore it in the design of their metrics. If this tool is meant to be used by those doing model calibration against paleo observations, then model

uncertainty and downscaling error needs to be explicitly accounted for in the metric. A few of my issues can be addressed by making the package more flexible to handle user choices of metrics (eg implemented by documentation of how to change the metric).

*We hope to have addressed the flaws in the algorithm, many of which we believe to be miscommunication on our part in the paper and addressed by some rewriting of the model-code. These are outlined below. As stated above, we outline model uncertainty to clarify for non-ice sheet modellers (i.e. those who collect geochronological data). We also think it is important to outline this uncertainty when making a comparison tool.*

*ATAT now runs from the command line, to better accommodate batch processing. ATAT outputs all metrics, as they are quick to calculate. This output is shown in the updated Figure 5, which now documents the new metrics designed to account for margin position and vertical uncertainty.*

I also agree with Evan Gowan's suggestion to significantly shorten the model uncertainty section. When I first read the paper, I expected all the detailed uncertainty discussion to lead to a detailed approach to handling model and data uncertainty. Given that these challenging aspects of model-data comparison are ignored in part (or in whole for model and downscaling uncertainty), I see no rationale for such detailed attention in this paper.

*We have shortened the length of this discussion, but retain the section as we think that understanding the uncertainty of the model is important when comparing to data. Uncertainty handling will come with ensemble design, the tool asks which ensemble member fits the data best.*

*We have also changed the code to deal with some downscaling uncertainty, in margin position and ice sheet elevation. Our method for dealing with this is now stated on lines 411-422.*

Lines 346-347: Samples for cosmogenic dating in glacial geology contexts are generally gathered in non-singular quantities for a given local (given all the uncertainties with inheritance). Consider a grid cell with two  $^{10}\text{Be}$  samples that have very little overlap in their age PDFs. This cannot be represented by a single Gaussian PDF, so I don't see how this interpolated single age approach can work for this context unless non-Gaussian PDF's are permitted (for which there is no indication).

*We addressed the issue of which date to choose for a cell in our response to Reviewer 1, and have strengthened our point, that not all dates are equal and this requires expert judgement, in lines 368-371.*

*It is true that non-gaussian dates occur. Our metrics are based upon whether the model hits a minimum (maximum) constraint in deglaciation (advance), meaning that all geochronological constraints are essentially one tailed depending upon stratigraphic context (see Figure 3). Therefore, the input error is a threshold beyond which model-data agreement does not occur (this is now clarified on lines 371-375). Therefore, if considering a skewed distribution a larger (or smaller) threshold should be defined by the user.*

*Future adaptations may account for more complex treatments of age probability.*

Lines 367-368: what range? one or two or 3 sigma? What if non-Gaussian?

*Our response to the issue of non-Gaussian distributions is stated above.*

*We now state that it is up to the user to define the level of sigma they wish to test (this may be different for radiocarbon, OSL or TCN ages) (lines 372-373).*

Lines 370-371: Does this take into account age uncertainty? If so, again to what sigma before rejection?

*There may be some miscommunication here, as we use the word error to refer to the uncertainty attached to a date (deliberately done to distinguish from model uncertainty). This is specifically input as a variable into ATAT, and we have clarified how to do this.*

Lines 373 and 376 and Eq 1: I don't follow the logic of the weighting scheme. Why should the weight be proportional  $d_i$ ? What if you have 2 equidistant adjacent cells with dates? Your weighting scheme assigns the same weight to a dated grid cell with one adjacent dated grid cell and a dated grid cell surrounded by equi-distant dated grid cells.

*We have changed the spatial weighting scheme to apply a search window which defines a local density of dated cells rather than a nearest neighbour distance. This is now outlined in the manuscript on lines 400-401.*

Lines 387-388: If I follow this correctly, the algorithm is outputting a binary agree-disagree result. If so, this should be changed to give a continuous metric (that can saturate to a large disagree result when disagreement is well beyond 3 sigma data + downscaling + some model uncertainty. Continuous metrics are required for efficient sampling/calibration algorithms. You will likely start with a bunch of "bad" models, and you need to be able to decipher which are less bad. If my interpretation of the metric is incorrect, then the description needs to be improved.

*ATAT outputs several metrics (these are listed at the bottom of Figure 5, and demonstrated at the bottom of Table 4 which seemed to be missing from our original submission). These include both continuous and non-continuous (agree/disagree) metrics. All metrics are output into a .csv file at the end of the comparison, which is named after the simulation name and whether deglacial or advance dates are being tested. Different users of the tool may want to use different metrics in different combinations. For example, to get rid of extremely poor simulations, it might be worth checking the percentage of sites covered. With better simulations, it may be worth checking the wRMSE of sites within dated error. It is also important keep the agree/disagree metric for the following reason: you may do 100 simulations of a palaeo ice sheet and keep getting the same sites that disagree. This may warrant investigation of the erroneous sites and re-evaluation of the data. This logic is stated in the text lines 299-307 and restated is now restated in the introduction (lines 80-84).*

Lines 389-406: Equations 2 and 3 don't take into account dating uncertainty, and are therefore inappropriate.

*We apply the RMSE to all dates to indicate how close to the observations the model is i.e. to develop a continuous metric. We also produce a metric which limits to only those data which have passed the original agree/disagree criteria. This is now clarified in the manuscript (lines 457-459).*

The comparison should also take into account elevation. If the modelled contemporaneous ice surface is below the elevation of the dated sample, then there is datapoint-model consistency even though ice is present contrary to what the presented algorithm would indicate. Given the coarse topography near the present-day margin of Greenland, for instance, elevation needs to be accounted for.

*We agree, and have now included an elevation consideration in the code and in the text. This helps resolve thinning issues for dates on trimlines or possible nunataks. Thank you for suggestion. This is now documented in the manuscript on lines (414-422).*

The algorithm also lacks consideration of subgrid/downscaling issues. Eg, for an ice marginal gridcell on a 25km grid, one would infer the actual subgrid margin to be somewhere within the gridcell since the next beyond margin gridcell has 0 mean ice thickness, and therefore 0 ice throughout. The easiest way to address this is to have a metric that takes into account proximity of the ice margin as well. This spatial proximity accounting is also important for model calibration to extract a continuous measure that can differentiate between two "bad" models.

*This is a great suggestion and something we had overlooked, thank you. We now include a separate metric that accounts for this uncertainty by applying a perimeter surrounding the originally identified margin. This is stated in the manuscript on lines 411-414.*

Lines 421-422: So by this logic, a model that was within 1 sigma of all but 2 data points and in the rejection region for those 2 datapoints (lets say out of 1000 datapoints) would be worse than a model that was only within 2 sigma everywhere with no data-points in the temporal rejection region ????

*Apologies, this is a miscommunication on our part. By "first filter" we meant to identify the worst model runs (e.g. those that do not glaciate over say 50% of the dated sites). We have clarified this in the text (lines 462-466).*

I would recommend inclusion of an in-line documented sample run script (ie that could be executed with a single command). Model data comparison in generally involve large ensembles, so a script that could be run in a loop would make this more accessible to users.

*We have redesigned the script to be run from the command line. An example of how to execute the script is included in the script header and in the instructions contained in section 6.*

The design of the comparison output needs more thought for use in ensemble comparisons. A summary file should be generated that for each line starts with a model run ID and then includes the summary metric values for that run. The tool should come with an looping script to cycle over model runs from some file list.

*A summary output file is produced every time ATAT is run and we have adapted the script to be run from a command line in order that batch processing can be done (e.g. from a shell script).*

Small corrections

Line 201: should mention even state-of-the-art GCMs still have relatively # large uncertainties for this context (just need to consider the spread across PMIP 3 submissions)

*This is now noted (lines 207-208).*

Line 490: English is broken.

*Now corrected.*

Lines 508-509: There is no way the uncertainties in a paleo cycle ice sheet model can be honestly represented by even a thousand model runs if one is claiming "full model evaluation".

*We have rephrased accordingly (lines 553-554).*

# ATAT 1.01, an Automated Timing Accordance Tool for comparing ice-sheet model output with geochronological data

Jeremy C. Ely<sup>1</sup>, Chris D. Clark<sup>1</sup>, David Small<sup>2</sup> and Richard C.A. Hindmarsh<sup>3</sup>

<sup>1</sup>Department of Geography, The University of Sheffield, Sheffield, S10 2TN, UK

<sup>2</sup>Department of Geography, Durham University, Durham, DH1 3LE, UK

<sup>3</sup>British Antarctic Survey, High Cross, Madingley Road, Cambridge, CB3 0ET, UK

Correspondence to: Jeremy C. Ely (j.ely@sheffield.ac.uk)

**Abstract.** Earth's extant ice sheets are of great societal importance given their ongoing and potential future contributions to sea-level rise. Numerical models of ice sheets are designed to simulate ice sheet behaviour in response to climate changes, but to be improved require validation against observations. The direct observational record of extant ice sheets is limited to a few recent decades, but there is a large and growing body of geochronological evidence spanning millennia constraining the behaviour of palaeo-ice sheets. Hindcasts can be used to improve model formulations and study interactions between ice sheets, the climate system and landscape. However, ice-sheet modelling results have inherent quantitative errors stemming from parameter uncertainty and their internal dynamics, leading many modellers to perform ensemble simulations, while uncertainty in geochronological evidence necessitates expert interpretation. Quantitative tools are essential to examine which members of an ice-sheet model ensemble best fit the constraints provided by geochronological data. We present an Automated Timing Accordance Tool (ATAT version 1.01) used to quantify differences between model results and geochronological-data on the timing of ice sheet advance and/or retreat. To demonstrate its utility, we perform three simplified ice-sheet modelling experiments of the former British-Irish Ice Sheet. These illustrate how ATAT can be used to quantify model performance, either by using the discrete locations where the data originated together with dating constraints or by comparing model outputs with empirically-derived reconstructions that have used these data along with wider expert knowledge. The ATAT code is made available and can be used by ice-sheet modellers to quantify the goodness of fit of hindcasts. ATAT may also be useful for highlighting data inconsistent with glaciological principles or reconstructions that cannot be replicated by an ice sheet model.

## 1 Introduction

Numerical models have been developed which simulate ice sheets under a given climate forcing (e.g. Greve, 1995; Rutt et al., 2009; Pollard and DeConto, 2009; Winkelmann et al., 2011; Gudmundsson et al., 2012; Cornford et al., 2013; Pattyn, 2017). When driven by future climate scenarios, these models are used to forecast the fate of the Antarctic and Greenland ice sheets (e.g. Seddik et al., 2012; DeConto and Pollard, 2016), providing predictions of their potential contribution to future sea level rise. However, incomplete knowledge of ice physics, boundary conditions (e.g. basal topography) and parameterisations of physical processes (e.g. basal sliding, calving), as well as the difficulty of predicting future climate, lead to uncertainty in these predictions (Applegate et al., 2012; Briggs et al., 2014; Ritz et al., 2015). Observations of ice marginal fluctuations (decades) and the processes of ice calving, flow or melting (subaerial or submarine) that facilitate or drive such variations, provide a powerful means to

37 understand the processes leading to the possibility of deriving new formulations that improve the realism of  
38 modelling. However, the short-time span (decades) of these observations limits their being used to constrain,  
39 initialise or validate modelling experiments (Bamber and Aspinall, 2013). Conversely, palaeo-ice sheets,  
40 especially from the last glaciation (~21,000 years ago), left behind evidence which provides the opportunity to  
41 study ice sheet variations across timescales of centuries to millennia, albeit with increased uncertainty in exact  
42 timing.

43 Numerous modelling studies have aimed to simulate the growth and decay of palaeo-ice sheets, producing  
44 hindcasts of ice-sheet behaviour (e.g. Boulton and Hagdorn, 2006; Hubbard et al., 2009; Tarasov et al., 2012;  
45 Gasson et al., 2016; Patton et al., 2016). Results from these hindcasts may be compared with empirical data  
46 recording ice sheet activity, so as to discern which parameter combinations produce results that best replicate the  
47 evidence of palaeo-ice sheet activity. Three classes of data are of particular use for constraining palaeo-ice sheets;  
48 (i) geomorphological data, (ii) relative sea level history, and (iii) geochronological data. Ideally, all three classes  
49 of data should be used to quantify the goodness of fit of a hindcast.

50 Geomorphological evidence comprises the landforms created by the action of ice upon the landscape, and can  
51 typically provide data on ice extent, recorded by moraines and other ice marginal landforms and on ice-flow  
52 directions recorded by subglacial landforms such as drumlins. Such landforms can be used to decipher the pattern  
53 of glaciation (e.g. Kleman et al., 2006; Clark et al., 2012; Hughes et al., 2014). Two tools have already been  
54 developed which can compare modelled ice margins and flow directions to the geomorphological evidence base  
55 (Napieralski et al., 2007).

56 Relative sea level data provides information regarding the mass-loading history of an ice sheet. Palaeo-ice-sheet  
57 model output is often evaluated against relative-sea-level data by use of glacio-isostatic adjustment models (e.g.  
58 Tushingham and Peltier, 1992; Simpson et al., 2009; Tarasov et al., 2012; [Auriac et al., 2016](#)).

59 Geochronological evidence attempts to ascertain the absolute timing of ice advance and retreat using dated  
60 material (e.g. organic remains dated by radiocarbon measurement) found in sedimentary contexts interpreted as  
61 indicating ice presence or absence nearby. It enables reconstruction of the chronology of palaeo-ice sheet growth  
62 and decay (Small et al., 2017) and is the underpinning basis for empirically-based ice sheet margin reconstructions  
63 (e.g. Dyke, 2004; Clark et al., 2012; Hughes et al., 2016). Although widely used in empirical reconstruction of  
64 palaeo-ice sheets, geochronological data has rarely been directly compared with ice sheet model output (although  
65 see Briggs and Tarasov, 2013). Such a comparison could be useful both for constraining ice-sheet model  
66 uncertainty and for identifying problems with the geochronological record. For example, a poor fit between model  
67 output and empirical data on timing could inform on the validity of a numerical model (or its parameterisation),  
68 or it could provide a physical basis for questioning the plausibility of empirically-driven interpretations or specific  
69 lines/data points of evidence given that they are associated with inherent uncertainties. In order to maximise the  
70 benefit to all users, any comparisons between palaeo-ice sheet model output and empirical data should ideally  
71 consider the inherent uncertainties of both.

72 Given the wide availability of compilations of geochronological data (e.g. Dyke, 2004; Hughes et al., 2011;  
73 Hughes et al., 2016), as well as the proliferation of ice sheet models (e.g. Greve, 1995; Rutt et al., 2009; Pollard  
74 and DeConto, 2009; Winkelmann et al., 2011; Gudmundsson et al., 2012; Cornford et al., 2013; Pattyn, 2017), a  
75 convenient, reproducible and consistent procedure for comparison should be of great utility to the palaeo-ice sheet  
76 community. The typical volume of geochronological constraints (several thousands) for a palaeo ice sheet and the

77 number of ensemble runs (several hundreds) from an ice sheet model make a visual matching of data and model  
78 output nearly impossible to accomplish, which is likely to explain the rarity of such comparisons. Here, we present  
79 an Automated Timing Accordance Tool (ATAT, version 1.01) ~~that compares geochronological data and ice-sheet~~  
80 ~~model output.~~ ATAT a systematic means for comparing ice-sheet model output with geochronological data,  
81 which quantifies the degree of fit between the two. To separate model uncertainty from data error, a single run of  
82 ATAT focuses on the error in geochronological data. However, through multiple comparisons against an ice-sheet  
83 model ensemble which considers model uncertainty, ATAT could be used as a basis for examining whether model-  
84 data mismatch is a consequence of inadequacies in either the model or data. The tool is in the form of a Python  
85 script and requires the installation of open-source libraries. ATAT is written to handle NETCDF data as an input,  
86 a format commonly used in ice sheet modelling and is also accessible from many GIS packages in which  
87 geochronological data can be stored and manipulated.

## 88 **2 Background**

89 Geochronological evidence and ice sheet model outputs are often independently used to reconstruct the timing of  
90 glaciological events. The two approaches are fundamentally different in nature and consequently produce  
91 contrasting data outputs. Thus, before describing our approach to comparing the two sets of data (ATAT), we first  
92 consider the nature of both geochronological data and ice-sheet model output to highlight the issues and potential  
93 difficulties associated with comparing the two and conceptualise a comparison procedure.

### 94 **2.1 Geochronological data**

95 The timing of palaeo-ice sheet activity has primarily been dated using three techniques: (i) radiocarbon dating;  
96 (ii) cosmogenic nuclide exposure dating, and (iii) luminescence dating (Figure 1). The utility of each method for  
97 determining the timing of palaeo-ice sheet activity has been extensively reviewed elsewhere (e.g. Fuchs and  
98 Owen, 2008; Balco, 2011; Small et al., 2017) and only a brief description is provided here. Radiocarbon dating  
99 uses the known rate of the radioactive decay of  $^{14}\text{C}$  to determine the time elapsed since the death of organic  
100 material (Libby et al., 1949; Arnold and Libby, 1951; Figure 1). For palaeo-glaciological purposes, the dated  
101 organic material (e.g. shells, mosses, plant remains) is usually taken from basal sediments overlying and closely  
102 associated with a glacial deposit in order to determine a minimum deglaciation age (e.g. Heroy and Anderson,  
103 2007; Lowell et al., 2009); ice is interpreted to have retreated from this site some short time prior to this age.  
104 Where organic matter is either reworked within or is located directly beneath a glacial deposit, it can be used to  
105 constrain the maximum age of glacial advance (e.g. Brown et al., 2007; Ó Cofaigh and Evans, 2007); advance  
106 happened sometime after this age. Cosmogenic nuclides (e.g.  $^{10}\text{Be}$ ,  $^{26}\text{Al}$  and  $^{36}\text{Cl}$ ) are produced by the  
107 interaction of secondary cosmic radiation in minerals, such as quartz, within materials exposed at the Earth's  
108 surface (Figure 1). Samples are generally taken from glacially-transported boulders, morainic boulders and  
109 glacially modified bedrock, all of which have ideally had signals from any previous exposure history removed by  
110 glacial erosion. Cosmogenic nuclide dating is thus used to determine the duration of time a sample has been  
111 exposed at the Earth's surface by determination of the concentration of cosmogenic nuclides within that sample.  
112 Luminescence dating can determine the age of a deposit by measuring the charge accumulated within minerals.  
113 This charge accumulates in light-sensitive traps within the crystal lattice due to ionizing radiation produced by

114 naturally occurring radioactive elements (e.g. U, Th, K). Luminescence dating determines the time elapsed since  
115 the last exposure of the mineral to sunlight; this exposure acts to reset the signal (Figure 1). As subglacial deposits  
116 are unlikely to have been exposed to light before burial, and therefore contain signals accumulated prior to  
117 deposition, luminescence dating within palaeo-glaciology is typically applied to ice marginal sediments, or those  
118 which overly glacial sediments (e.g. Duller, 2006; Smedley et al., 2016; Bateman et al., 2018). All  
119 geochronological techniques record the absence of grounded ice. They therefore provide either maximum or  
120 minimum ages of a glaciological event, depending upon the stratigraphic setting. Table 1 outlines a commonly  
121 used system used to classify geochronological data by stratigraphic setting (Hughes et al., 2011; 2016).

122 The retreat/advance (ice-free) ages provided by the three geochronometric techniques are all affected by  
123 systematic and geological uncertainties (Small et al., 2017). Systematic uncertainties originate from the tools and  
124 techniques used to derive the date, such as laboratory instruments and sample preparation, and are accounted for  
125 in the quoted errors that accompany a date. Geological uncertainties are caused by the geological history of a  
126 sample, before, during and after a glacial event (e.g. Lowe and Walker, 2000; Lukas et al., 2007; Heyman et al.,  
127 2011). Such influences may leave little or no evidence of their effect upon a sample and are thus hard to quantify.  
128 The relationship between a dated sample and the glacial event it indicates is the largest potential source of  
129 uncertainty in geochronological data and is primarily bounded by the ability of the investigator to find and  
130 associate dateable material to the glacial event of interest. Since all geochronological techniques measure the  
131 absence of ice, expert inference must be made, and are influenced by the availability of information (stratigraphic  
132 or otherwise) at a study site; they may be open to change (e.g. new radiocarbon calibrations, new cosmogenic  
133 isotope production rates). Furthermore, in the cases of luminescence and radiocarbon dating, there can be an  
134 unknown duration since glacial occupation of an area and the deposition of dateable material. These factors mean  
135 it is necessary to consider the quality of dates for ascertaining the timing of the glacial event in question (Small et  
136 al., 2017).

137 Numerous geochronological studies have sought to ascertain the timing of palaeo-ice sheet activity at sites, leading  
138 to compilations of geochronological data which bring together hundreds to thousands of published dates (e.g.  
139 Dyke et al., 2002; Livingstone et al., 2012; Hughes et al., 2011; 2016). Despite the growing number of reported  
140 dates, they are still insufficient in number and spatial spread to define, on their own, the time-space envelope of  
141 the shrinking ice sheet. Techniques to interpolate geochronological information between sites are required. The  
142 most commonly used technique is empirical ice sheet reconstruction (e.g. Dyke, 2004; Clark et al., 2012), whereby  
143 expert assessments of the geochronological and geomorphological record are used together to create ice-sheet  
144 wide isochrones of ice-sheet margin position and flow configuration. A recent advance in this method has been  
145 the inclusion of confidence envelopes for each isochrone, documenting possible maximum, likely and minimum  
146 extents (Hughes et al., 2016). Further techniques for spatiotemporally interpolating geochronological data include  
147 Bayesian sequence modelling (e.g. Chiverrell et al., 2013; Smedley et al., 2017), in which collections of deglacial  
148 ages are arranged in spatial order determined by a priori knowledge of geomorphologically-informed ice flow and  
149 retreat patterns (e.g. Gowan, 2013). Such techniques provide viable methods for producing ice-sheet wide  
150 chronologies, filling in information in locations where geochronological data may be sparse.

## 151 2.2 Ice sheet model output

152 Ice-sheet models solve equations for ice flow over a computational domain, for a given set of input parameters  
153 and boundary conditions, to determine the likely flow geometry and extent of an ice sheet. Typically, ice-sheet  
154 models run using finite difference techniques on regular grids (e.g. Rutt et al., 2009; Winkelmann et al., 2011).  
155 Ice-sheet models that utilise adaptive meshes (e.g. Cornford et al., 2013) and unstructured meshes also exist (e.g.  
156 Larour et al., 2012) and the results from such models can be interpolated onto spatially regular grids. The spatial  
157 resolution of an ice-sheet model depends upon the computational resources available, and the spatial resolution  
158 of available boundary conditions. Continental-scale models of palaeo-ice sheets have typical spatial resolution of  
159 tens of kilometres (e.g. Briggs and Tarasov, 2013; DeConto and Pollard, 2016; Patton et al., 2016), though parallel,  
160 high-performance computing means higher resolutions are possible (e.g. 5 km in Golleger et al., 2013 and  
161 Seguinot et al., 2016). The temporal resolution of ice sheet model output is ultimately limited by the time-steps  
162 imposed by the stability properties of the numerical schemes solving the ice-flow equations. Given that these  
163 stable time-steps can be sub-annual, output frequency is mostly predetermined by the user (typically decades to  
164 centuries), and as such is constrained by available disk-storage. Ice-sheet models therefore produce spatially  
165 connected predictions of ice-sheet behaviour such as advance and deglaciation (e.g. Table 1) across gridded  
166 domains at various temporal and spatial resolutions.

167 The stress fields imposed upon ice can be fully described by solving the Stokes equations. Indeed, ‘full Stokes’  
168 models which do so have been tested (Pattyn et al., 2008) and used to simulate ice sheets (e.g. Seddik et al., 2012).  
169 However, fully solving the Stokes equations over the spatio-temporal scales relevant to palaeo-ice sheet  
170 researchers remains beyond the limit of currently available computational power. This problem is exacerbated by  
171 the need to run multi-parameter valued ensemble simulations to account for model uncertainty over multi-  
172 millennial and continental-scale domains. This means that palaeo-ice sheet modelling experiments rely upon  
173 approximations of the Stokes equations (see Kirchner et al., 2011 for a discussion), such as the shallow ice  
174 approximation (SIA) and shallow shelf approximation (SSA). The choice of ice-flow approximation used within  
175 a model has implications for the capability of models to realistically capture aspects of ice sheet flow (Hindmarsh,  
176 2009; Kirchner et al., 2011; 2016), and in turn influences the nature of the model output produced. For instance,  
177 the SIA is not applicable for ice shelves, therefore SIA-based models do not produce modelled ice shelves (e.g.  
178 Glimmer; Rutt et al., 2009). Therefore, the timing of deglaciation in an SIA model can be determined as the point  
179 at which ice thickness in a cell becomes zero or thinner than the flotation thickness, ~~whereas in a SSA or higher-~~  
180 ~~order model the location and movement of the grounding line must be determined. In a model which predicts the~~  
181 ~~location of ice shelves (e.g. a SSA or higher-order model), the location and movement of the grounding line must~~  
182 ~~be determined in order to calculate the modelled retreat or advance age. Such models typically produce a ‘mask’~~  
183 ~~variable from which the extent of grounded ice can be determined (e.g. PISM; Winkelmann et al., 2011).~~

184 Though ice sheet models produce output which is consistent with model physics, there are many sources of  
185 uncertainty involved with ice sheet modelling. This uncertainty has two main sources: (i) parameterisations, and  
186 (ii) boundary conditions. Where a process is too complex (e.g. calving) or occurs at too small a scale (e.g.  
187 regelation) to be captured by an ice sheet model, it is often simplified and parameterised. Associated with each  
188 parameterisation are a set of parameters, the values of which are either unknown, or thought to vary within some  
189 plausible bounds, ~~and. This leads to an associated uncertainty when choosing these input parameters,~~ which can  
190 either be constant or spatially and temporally variable across a domain. An example of a process which is often

191 parameterised is basal sliding. This parameterisation is often done through the implementation of a sliding law  
192 (e.g. Fowler, 1986; Bueler and Brown, 2009; Schoof, 2010), which relates the basal shear stress to the basal  
193 velocity (Fowler, 1986). ~~Exact determination of basal shear stress requires knowledge of basal roughness,  
194 hydrological conditions and, where present, sediment rheology. These terms~~ Parameters used to determine this  
195 relationship are often assigned or incorporated within a parameter, or prescribed by another model  
196 parameterisation (e.g. a subglacial hydrology model). Adding to the uncertainty in the absence of a single  
197 preferable sliding law, ice-sheet models often allow the user to choose between different sliding law  
198 implementations.

199 Boundary conditions, the values prescribed at the edge of the modelled domain, also introduce uncertainty into  
200 ice-sheet models. For contemporary ice sheets, there is a large uncertainty in the basal topography (e.g. Fretwell  
201 et al., 2013). This is less of a problem for the more accessible beds of palaeo-ice sheets. However, accurately  
202 accounting for the evolution of this bed topography over the course of a glaciation requires a model of isostatic  
203 adjustment (Lingle and Clark, 1985; Gomez et al., 2013).

204 A very large source of uncertainty for modelling palaeo-ice sheets is the climate used to drive them (Stokes et al.,  
205 2015), as indeed is the case for forecasts of contemporary ice sheets (e.g. Edwards et al., 2014). Owing to the  
206 computational resources required and technical challenges, few palaeo-ice sheet models are coupled with climate  
207 models. ~~This uncertainty over past climate is reflected in the large range of outputs produced by global circulation  
208 models which have tried to simulate the last glacial cycle (e.g. Braconnot et al., 2012).~~ Palaeo-ice sheet modellers  
209 have ~~mostly used offline methods to force their models with representations of palaeo-climate. used a range of  
210 methods to force their models, including~~ These include simple parameterisations (Boulton and Hagdorn, 2006),  
211 applying offsets derived from ice core records to contemporary climate (Hubbard et al., 2009) and scaling between  
212 present-day conditions and uncoupled global-circulation-model simulations at maximum glacial conditions  
213 (Gregoire et al., 2012; Gasson et al., 2016). Each approach ~~has advantages and disadvantages, but, most  
214 importantly, is also~~ associated with an inherent uncertainty. When this uncertainty is accounted for, the range of  
215 possible climates produces numerous ice sheet outputs.

216 There is another cause of ice-sheet models not being able to accurately predict the evolution of ice-sheets, which  
217 is the presence of instabilities – we use this term in the technical sense of a small perturbation in leads to the whole  
218 ice-sheet system amplifying this small perturbation to the extent it can leave a mark in the geological record. A  
219 classic example of this in ice-sheet dynamics is the marine ice-sheet instability (MISI), first discussed in the 1970s  
220 (Hughes, 1973; Weertman, 1974, Mercer, 1978) and more recently put on a sounder mathematical footing (Schoof  
221 2007, 2012).

222 The MISI actually refers to an instability in grounding-line (GL) position on a reverse slope, where the water  
223 depth is shallowing in the direction of ice flow. Since ice flux increases with ice thickness, a straightforward  
224 argument leads to the conclusion that if the GL advances into shallower water, the efflux will decrease, the ice  
225 sheet will gain mass and the advance continue. If, on the other hand, the GL retreats, the ~~efflux will increase, the  
226 ice-sheet will lose mass and the retreat continue. The latter process led to concerns that the retreat of Antaretic  
227 and Greenlandic ice sheets would cause several metres of sea level rise over one or two centuries. Schoof  
228 (2007, 2012) showed that the MISI was in accordance with the understanding and use of the word ‘instability’ by  
229 physicists and mathematicians.~~

230 In principle, given the right parameterisations and basal topography, ice-sheet models should be able to predict  
231 the ‘trajectory’ of GL migration arising as a consequence of the MISI. However, the MISI is one of the class of  
232 instabilities that lead to poor predictability; certain small variations of parameters and specifications will lead to  
233 large-scale changes in the ‘trajectory’, in this case the retreat history. A well-known analogy is the ‘butterfly  
234 effect’, which originated in atmospheric modelling work (Lorenz, 1963); the butterfly effect is concerned with the  
235 consequences of the statement “small causes can have larger effects”. Recent work has also shown that additional  
236 physical processes, such as ice-shelf buttressing (Gudmundsson, 2012) and the effect that the gravitational pull of  
237 ice-sheets has on sea level (Gomez et al., 2012) have additional effects on grounding line stability. Given that  
238 most of the palaeo-ice sheets during the last glacial cycle had extensive marine margins and overdeepened basins,  
239 with isostatic adjustment creating further zones of reverse slope, capturing grounding line processes is important  
240 for simulating these ice-sheets.

241 ~~Schoof’s theory was for a very straightforward marine ice sheet configuration —no buttressing, ice motion all by~~  
242 ~~sliding, isothermal, but its accuracy was confirmed by a large group of researchers running their models for this~~  
243 ~~simple configuration (Pattyn et al., 2012). Schoof (2012) showed that for his configuration, the existence of a~~  
244 ~~reverse slope was sufficient condition for the MISI to exist. However, later work (Gudmundsson, 2012; Gomez~~  
245 ~~et al., 2012) presented results showing that stable GL positions could exist on a reverse slope if extra physical~~  
246 ~~processes were included (Gudmundsson introduced buttressing, Gomez et al. included the effect of lateral~~  
247 ~~gravitational attraction on sea-level). Their results indicated that the reverse slope was not a sufficient condition~~  
248 ~~for instability.~~

249 ~~Most of the palaeo ice sheets at the LGM had extensive marine margins at their polar edges, certainly the~~  
250 ~~Laurentide, Fennoscandian and British-Irish ice-sheets, and the present-day bathymetry of the seas around North~~  
251 ~~America and Europe strongly suggests that a reverse slope would have existed —moreover, isostatic adjustment~~  
252 ~~under the weight of the ice sheets would have created further extensive zones of reverse slope. There are data~~  
253 ~~indicating rapid retreat along some zones of reverse slope in palaeo-ice sheets, which leads to the question of how~~  
254 ~~accurately we should expect ice-sheet models to be able to reproduce the observed retreat rates in the presence of~~  
255 ~~physical instability. Schoof’s progress is very recent, so the necessary ensemble runs have yet to be carried out by~~  
256 ~~researchers focussing on the relationship between the presence of the MISI and the amplification of data~~  
257 ~~uncertainties or physics errors/over simplifications (as placed in the models).~~

### 258 **2.3 Considerations when comparing geochronological data and ice-sheet model output**

259 Sections 2.1 and 2.2 make it clear that several factors must be considered in order to satisfactorily compare  
260 geochronological data and ice-sheet model output (Table 2). Most critically, the two datasets involved in any  
261 comparison have varying spatial properties. Raw geochronological data is unevenly distributed and located at  
262 specific points, with horizontal position accurate to a metre or so; such data may be used to plot ice-margin  
263 fluctuations of the order of tens of kilometres (Figure 2C). Ice-sheet models typically produce results on evenly-  
264 spaced points (at ~5 km to 20 km resolution) that are distributed over and beyond the maximum area of the palaeo-  
265 ice sheet (Table 2; Figure 2B). Consequently, in comparing the two, a choice must be made; either  
266 geochronological data should be gridded (coarsened) to the resolution of the ice-sheet model, or the ice-sheet  
267 model results must be interpolated to a higher resolution. Both options have drawbacks, as the former removes  
268 spatial accuracy from geochronological data while the latter relies upon interpolation beyond model resolution

269 and, more seriously, model physics. A second problem lies in the spatial organisation of the data (Table 2). Ice-  
270 sheet models produce a regular grid of data (Figure 2B), meaning that no location is more significant than any  
271 other when comparing the modelled deglacial chronology with that inferred from geological data. Conversely,  
272 owing to the uneven distribution of raw geochronological data, some regions of a palaeo-ice sheet may be better  
273 constrained than others (Figure 2C). As noted by Briggs and Tarasov (2013), any comparison that does not treat  
274 the uneven spatial distribution of geochronological data may favour sites where numerous dates exist over more  
275 isolated locations. One approach to overcoming these disparities is to use an interpolation scheme (e.g. empirical  
276 reconstruction, Bayesian sequence) on the raw geochronological data. This produces a geochronological  
277 framework by combining evidence on pattern and timing to yield a distribution that is spatially more uniform and  
278 a spatial resolution similar to that of palaeo-ice sheet model output (Figure 2D).

279 The temporal intervals between and precision of geochronological data and ice sheet model output also vary  
280 (Table 2). The time intervals between geochronometric data are determined by the number of available  
281 observations, and precision determined by sources of uncertainty. Conversely, ice sheet models produce output at  
282 regular intervals and are temporally exact, which is to be contrasted with 'correct'. Since the output interval of an  
283 ice-sheet model is generally determined by the user (see Section 2.2) it is pertinent to consider an appropriate  
284 time-interval of ice-sheet model output for comparison with geochronological data. For example, radiocarbon  
285 dates have precision typically in the order of hundreds of years but do not directly constrain ice extent, whilst  
286 empirically reconstructed isochrones are typically produced for thousand-year time-slices (e.g. Hughes et al.,  
287 2016). In reality, ice-sheets may respond to events at faster time-scales than this, but in the absence of internal  
288 instabilities (e.g. MISI) palaeo-ice sheet models are ultimately limited by the temporal resolution of the available  
289 climate forcing data. Thus, to gain insight into controls on palaeo-ice sheet behaviour, it may be necessary to  
290 create model output with a greater (centurial) temporal resolution than the uncertainty associated with  
291 geochronology.

292 Both geochronological data and ice-sheet model output have sources of uncertainty which must also be considered  
293 when comparing the two. For geochronological data, uncertainty is typically expressed as a standard deviation  
294 from the reported age, and are therefore easy to consider when comparing to an ice sheet model. For ice-sheet  
295 models, individual model runs do not currently express uncertainty, and it is only when multiple, ensemble, runs  
296 which systematically vary parameters and boundary conditions are conducted that uncertainty in all output  
297 variables can be expressed. Having said this, statistical techniques exist to derive probability distribution functions  
298 for individual quantities (e.g. Ritz et al., 2015). Such ensemble runs typical comprise hundreds to thousands of  
299 individual runs (Tarasov and Peltier, 2004; Robinson et al., 2011). Given the volume of data this produces, one  
300 appealing application of a quantitative comparison between geochronological data and ice sheet model output  
301 would be to act as a filter for scoring ice-sheet model runs and reducing predictive uncertainty by only using the  
302 parameter combinations that were successful. However, if all possible parameters have been modelled, (i.e. the  
303 full 'phase-space' of the model has been explored (cf. Briggs and Tarasov, 2013)), and very few (or no) model  
304 runs conform to a certain set of geochronological data or an empirical reconstruction, this may provide a basis to  
305 question aspects of the evidence (e.g. re-examining the stratigraphic context of a dated sample site or questioning  
306 the basis of the reconstructed isochrone). Of course, a third possibility that both data and model are incorrect  
307 cannot be excluded.

308 We therefore suggest that any comparison between ice-sheet model experiments and geochronological data should  
309 consider:

- 310 i) That both ice-sheet models and geochronological data have inherent uncertainties;
- 311 ii) That geochronological data typically provide a constraint on just the absence of ice; such that ice must have  
312 withdrawn from a site sometime (50 years? 500 years? 5000 years?) prior to the date (which can be any point  
313 within the full range of the stated uncertainty). It is thus a limit in time and not a direct ~~fi~~measure of glacial  
314 activity. Figure 3 illustrates this for advance and retreat constraints. It is most often the case that dated material is  
315 taken close to the stratigraphic boundary or landform representing ice presence, in which case a date might be  
316 considered as a 'tight constraint' (e.g. the ice withdrew and very soon afterwards (50 years) marine fauna colonised  
317 the area and deposited the shells used in dating). Sometimes however there may have been a large (centuries to  
318 millennia) interval of time between the withdrawal and the age of the shell chosen as a sample, in which case the  
319 date will provide a 'loose' limiting constraint; it might be much younger than ice retreat (Figure 3).
- 320 iii) There is inherent value to the expert interpretation of stratigraphic and geomorphological information, meaning  
321 an ice-free age reported for a site is likely as close as possible (tight constraint) to a glacial event. However, this  
322 interpretation could be subject to change;
- 323 iv) Geochronological data exist as spatially distributed dated sites (e.g. Figure 2C) which can be built into a  
324 spatially coherent reconstruction (e.g. Figure 2D);
- 325 v) A great input uncertainty in a palaeo-ice sheet model is the climate, which can lead to changes in the spatial  
326 extent and timing of ice sheet activity.
- 327 vi) A factor which requires further investigation is the relationship between the operation of a physical instability  
328 (e.g. the MISI) and the practical ability of models to predict retreat or advance rates; the presence of an instability  
329 can result in extreme sensitivity to parameter ignorance or over-simplified model physics.
- 330 vii) Other uncertainties can also lead to variations in ice-sheet model results; these can be accounted for in an  
331 ensemble of hundreds to thousands of simulations.

332 Given the above, it is unlikely that a single procedure could capture model-data conformity. ATAT therefore  
333 implements several ways of measuring data-model discrepancies and produces output maps (described in the  
334 following two sections) to help a user assess which model runs best agree with the available geochronological  
335 data. One approach is to transform the geochronological data points (x,y,t) to a gridded field (raster) that define  
336 age constraints of ice advance and another grid for retreat. Both of these data types also require an associated grid  
337 that reports the uncertainty range as error (Figure 4). These age grids may then be quantitatively compared to  
338 equivalent grids (age of advance grid and age of retreat grid) derived from the ice sheet model outputs.  
339 Alternatively, one might prefer to compare model runs against the geochronological data (points) combined with  
340 expert-sourced interpretive geomorphological and geological data, in which age constraints from dated sites have  
341 been spatially extrapolated using moraines and the wider retreat pattern. In this case ATAT allows the model  
342 outputs to be compared to the 'lines on maps' type of reconstruction subsequent to conversion from age isolines  
343 to a grid of ages (Figure 4).

344 **3. Description of tool**

345 ATAT is written in Python, and utilises several freely available modules. Access to these modules may require a  
346 Python package manager, such as 'pip' or 'anaconda'. ATAT can therefore be run from the command line on any  
347 operating system, or by using a Python interface such as IDLE.

348 **3.1 Required data and processing**

349 ATAT requires two datasets as an input: (i) an ice-sheet model output; and (ii) gridded geochronological data.  
350 Table 3 provides the required variables and standard names for each dataset. In order to determine the advance  
351 age or deglacial age predicted by the ice sheet model, ATAT requires either an ice thickness (where the model  
352 does not produce ice shelves) or a grounded ice-mask variable (where ice shelves are modelled). In the latter case,  
353 the user is asked to define the value which represents grounded ice.

354 Empirical advance and deglacial geochronological data (Table 1) require separate input files (NETCDF format),  
355 as model-data comparison for these two scenarios are run separately in ATAT. Table 1 and further references  
356 (Hughes et al., 2011; 2016; Small et al., 2017), provide information regarding identification of the stratigraphic  
357 setting of these two glaciological events as considered by ATAT. ATAT requires that geochronological data  
358 (advance or deglacial) are interpolated onto the same grid projection and resolution as the ice-sheet model before  
359 use. Though an imperfect solution to the problem of comparing grids of different resolution, (Section 2.3; Table  
360 2), this was preferred to the alternative solution of regridding an ice sheet model onto a higher resolution grid, as  
361 this may introduce the false impression of high resolution modelling sensitive to boundary conditions (e.g.  
362 topography) beyond the actual model resolution.

363 Preparation of the geochronological data to be the same format and grid resolution as the ice sheet model output  
364 requires use of a GIS software package such as ESRI ArcMap or QGIS. Users must define deglacial/advance ages  
365 based either upon the availability of geochronological data in a cell, or based upon an empirical reconstruction  
366 (Figure 4). These ages must be calibrated to a calendar which is the same as that output by the ice-sheet model (in  
367 our case the 365-day calendar in units of seconds since 1-1-1). Where there are no data (i.e. outside the ice-sheet  
368 limit), the grid value must be kept at 0. When multiple dates are contained within a cell, expert judgement is  
369 required to ascertain which date is most representative of the deglaciation of a region. The assembly of this  
370 geochronological database input into ATAT should consider the reliability of ages, removing outliers and  
371 unreliable ages (see Small et al. (2017) for a discussion of this issue). In a comparable manner, the attribution of  
372 error to each cell is also reliant upon expert interpretation. The magnitude of error may vary between the source  
373 of geochronological data and user choice for experimental design (e.g. 1, 2 or 3 sigma). A single error value must  
374 be given for each dated cell, corresponding to the maximum threshold beyond which it is unacceptable for a model  
375 prediction to occur (Figure 3). Given that ~~this creating this input data~~ may involve many expert decisions (e.g.  
376 which date has the relevant stratigraphic setting, which date(s) are most reliable?), this part of the process is not  
377 yet automated within ATAT. This data preparation stage is therefore the most time-consuming and user-intensive  
378 part of the process. However, users only need to define the data-based advance/deglacial grid once to compare to  
379 multiple model outputs. Future work should consider alternatives means of choosing dates and identifying outliers,  
380 such as Bayesian age modelling (e.g. Chivverell et al., 2013). The input data NetCDF file should also contain the  
381 variables latitude, longitude, base topography (the topography that the ice-sheet modelling is conducted on and  
382 the elevation of the geochronological sample (Table 3).

383 ATAT is called from a suitable python command-line environment, using several system arguments to define  
 384 input variables. Upon starting ATAT, the user is first asked to define whether they are testing a deglacial or advance  
 385 scenario (Table 1; Figure 5). Users must define whether they are testing a deglacial or advance scenario. ATAT  
 386 only considers the last time that ice advances over an area. Therefore, caution must be undertaken when defining  
 387 advance data in regions where multiple readvances occur, and users should consider limiting the time interval of  
 388 the ice sheet model tested when examining specific events (e.g. a well-dated readvance or ice sheet build-up). The  
 389 location of the file containing the geochronological data grid (e.g. Figure 5) is then required. From this file, the  
 390 age and error grids are converted to arrays. For the age data, null values are masked out using the numpys masked  
 391 array function. A second array that accounts for error is then created, the properties of which depends upon  
 392 whether a deglacial or advance scenario is being tested. For a deglacial scenario, a model prediction will be  
 393 unacceptable if the cell is ice-covered after the range of the date error is accounted for, but the cell may become  
 394 deglacial any time before this. Therefore, the associated error value is added onto the cell date, to create a  
 395 maximum age at which a cell must be deglacial by to conform to the ice sheet model (Figure 3). The opposite  
 396 is true for advance ages; ice can cover a cell any time after the date and associated error, but cannot cover the cell  
 397 before the date of the advance. In order to allow for advances which occur after the date and its error, associated  
 398 error is therefore subtracted from the date cell (Figure 3). To account for the uneven spatial distribution of dates,  
 399 a weighting for each date is then calculated based upon their spatial proximity. This weighting is used later when  
 400 comparing the data to the model output. To calculate this weighting ( $w_i$ ), ATAT defines a local spatial density of  
 401 dated values based upon a kernel search of 10 neighbouring cells, the Euclidian distance from each dated cell to  
 402 its nearest dated cell ( $d_i$ ) is calculated. The mean distance between dated cells ( $\bar{d}$ ) is then calculated, and the  
 403 weight of each location ( $w_i$ ) defined using Eq. (1):

$$w_i = \frac{d_i}{\bar{d}}$$

(1)

406 ~~The user is then asked to~~The user must define the path to the ice sheet model output, from which the modelled  
 407 deglacial age will be calculated and eventually compared to the data (Figure 4). The user ~~is also asked~~must also  
 408 define whether to base deglacial timing on an ice thickness or grounded extent mask variable (Table 2). If the user  
 409 selects thickness, the margin is defined by an increase from 0 ice thickness. For the mask, the user is also asked  
 410 to supply the number which refers to grounded ice extent. The timing of advance is then determined by the change  
 411 of a cell to this number (Figure 5). The margin position recreated by the ice-sheet model has a spatial uncertainty  
 412 due to downscaling issues and fluctuations which may occur between recorded outputs. To account for this, ATAT  
 413 calculates a second set of modelled deglacial ages, whereby the deglacial region at each modelled time output  
 414 is expanded to all cells which neighbour the originally identified deglacial or advanced over cells. Furthermore,  
 415 the spatial resolution of ice-sheet models typically means that the emergence of ice-free topography at the edge  
 416 or within an ice-sheet (e.g. in situations such as steep-sided valleys or nunataks) are poorly represented. To account  
 417 for this, ATAT firstly calculates the modelled ice-sheet surface at each time output by adding ice thickness to the  
 418 input base topography. Where the modelled surface elevation is below that of the sample elevation, these cells are  
 419 identified as being deglacial (Figure 5). The downscaling of topography onto ice-sheet model grids also  
 420 introduces a vertical uncertainty. This is accounted for in ATAT through calculating the difference between  
 421 sample elevation and the reference elevation. A second metric which identifies cells as having been deglacial  
 422 if they are also within this vertical uncertainty is also calculated (Figure 5).

Formatted: Space Before: 0 pt, After: 0 pt

423 **3.2 Model-data comparison**

424 Once the required variables have been retrieved from the NETCDF data and manipulated, ATAT compares the  
425 geochronological age and modelled age at each location (Figure 4). Firstly, the grid cells which have data are  
426 categorised as to whether there is model-data agreement, based on the criteria shown in Figure 3. Since all dating  
427 techniques only record the absence of ice, geochronological data provides only a one-way constraint on palaeo-  
428 ice sheet activity. For deglacial ages, deglaciation could occur any time before the geochronological data provided  
429 and within the error of the date, but deglaciation must not occur after the error of the date is considered (Figure  
430 3). For advance ages, advance must have happened after the date or within error beforehand, but palaeo-ice sheet  
431 advance cannot occur in the time period before that dated error (Figure 3). Once ATAT has determined whether  
432 each cell conforms to these criteria, a map is produced identifying at which locations the ice sheet model agrees  
433 with the geochronological data.

434 -Though the criteria described above and illustrated in Figure 3 allow for the identification of dates which conform  
435 to the predictions of an ice sheet model, they provide little insight into how close the timing of the model prediction  
436 is to the geochronological data. If these were the only criteria on which a model-data comparison was made, it  
437 could prove problematic. In an extreme case, one could envisage that all retreat dates are adhered to by a model  
438 run that deglaciates from a maximum extent implausibly rapidly (say 50 years!), and, given that we only have  
439 one-way constraints on deglaciation (Figure 3), this model run would conform to all modelled dates. Whilst the  
440 nature of geochronological data (being only able to determine the absence of ice) does not preclude such a  
441 scenario, this assumes that there is no inherent value to the expert judgement and stratigraphic interpretation of  
442 each date as being close to palaeo-ice sheet timing (cf. Small et al. 2017). Therefore, ATAT also determines the  
443 temporal proximity of the geochronological data and the model prediction. Firstly, a map of the difference between  
444 modelled and empirical ages is created (Figure 5). This enables the identification of dates which are a large  
445 distance away from the model prediction. Secondly, the route-mean square error (RMSE) is calculated using the  
446 Eq. (2):

447 
$$RMSE = \sqrt{\frac{1}{n} \sum_{i=1}^n (g_i - m_i)^2},$$
  
448 (21)

449 where n is the number of cells which contain empirical geochronological information, g\_i is the associated  
450 geochronological date, and m\_i is the model predicted age. The RMSE works well when the geochronological  
451 data is evenly spatially distributed, either from a reconstruction (i.e. isochrones) or a wealth of dates. ATAT also  
452 calculates a weighted RMSE (wRMSE), for situations where this is not the case (i.e. there is a paucity of dates  
453 that are not distributed evenly across the domain) using Eq. (3):

454 
$$wRMSE = \sqrt{\frac{1}{n} \sum_{i=1}^n ((g_i - m_i) * w_i)^2},$$
  
455 (22)

456 where w\_i is the spatial weighting factor, ~~determined in Eq. (1).~~ Both the RMSE and wRMSE are calculated for  
457 all dates, to create a metric that doesn't account for dating error but may give an indication of how close a model-  
458 run gets to dated cells, and also for those dates which where model-data agreement within dating error occurs to  
459 create a metric which does account for model-errordated regions which have different levels of conformity with

Formatted: Subscript

460 ~~the model output~~ (Figure 5). ATAT then produces a .csv file ~~containing all calculated with these~~ statistics per ice-  
461 sheet model output file. Given the complexity of data-model comparison, different statistics may have different  
462 uses. For instance, the percentage of covered dates may prove useful to identify the worst performing model runs  
463 (i.e. the bottom 50%) as a first filter of model runs, whilst the wRMSE of dates within error may be more  
464 convenient for choosing between ~~filtered~~ model runs. However, given the uncertainty in ice-sheet modelling it is  
465 likely that in an ensemble there will be no single model run which has significantly better metrics than others, so  
466 ATAT may best be used to choose members which pass a user-defined threshold of combined metrics.

#### 467 4. Application of tool

##### 468 4.1 Ice Sheet Model

469 To trial ATAT we used geochronological data and ice sheet modelling experiments from the former British-Irish  
470 Ice Sheet (BIIS). A vast quantity of previous research has produced a high density of dates (Hughes et al., 2011)  
471 which are being substantially augmented by the BRITICE-CHRONO project ([http://www.britice-](http://www.britice-chronology.group.shef.ac.uk/)  
472 [chronology.group.shef.ac.uk/](http://www.britice-chronology.group.shef.ac.uk/)). Along with an abundance of well documented landforms (Clark et al., 2017), this  
473 makes the BIIS a data-rich study area for empirical reconstructions and ice sheet modelling. Ongoing modelling  
474 work aims to capture the behaviour of the BIIS inferred from the geomorphological and geochronological record  
475 (see Clark et al., 2012 for a recent reconstruction). We do not expect our model to capture these specific details.  
476 Instead, the purpose of modelling in this paper is merely to illustrate the use of ATAT. We therefore restrict  
477 ourselves to simplified modelling experiments and show only three model runs (Experiments A, B and C), whereas  
478 a full ensemble experiment would contain hundreds or thousands of simulations.

479 Ice sheet modelling experiments were conducted using the Parallel Ice Sheet Model (PISM; Winkelmann et al.,  
480 2011). This is a hybrid SIA-SSA model, with an implementation of grounding line physics. It is therefore suited  
481 to modelling both the marine-based portions of the BIIS and the terrestrial realm. The model simulates the history  
482 of the BIIS from 40 ka to present. The model is run at 5 km resolution, with basal topography derived from the  
483 General Bathymetric chart of the Oceans ([www.gebco.net](http://www.gebco.net)). This is updated to account for isostatic adjustment  
484 using a viscoelastic Earth model (Bueler et al., 2007) and a scalar eustatic sea level offset based on the SPECMAP  
485 data (Imbrie et al., 1984). All three model runs, labelled A-C, had the same input parameters and boundary  
486 conditions, apart from climate forcing. We take a similar approach to Seguinot et al. (2016) in computing a climate  
487 forcing. Modern values of temperature and precipitation are perturbed by a proxy temperature record, in this case  
488 the GRIP ice core record (Johnsen et al., 1995). These are input into a positive degree day model to calculate mass  
489 balance (Calov and Greve, 2005). Input precipitation values are the same between experiments. To introduce  
490 variation between the experiments, temperature varies such that Experiment A is the equivalent of modern day  
491 values, Experiment B has values uniformly reduced by 1°C and Experiment C has values uniformly reduced by  
492 2°C. All other parameters and forcings are equal between experiments. This simple approach to climate forcing  
493 here used for demonstration purposes only, and does not capture the changes to atmospheric and oceanic  
494 circulation patterns that occur during a glacial cycle.

495 The maximum extent of ice for each experiment is shown in Figure 6 and the timing of advance and retreat is  
496 shown in Figure 7. Potentially unrealistic ice sheets occur in the North Sea, perhaps due to the choice of domain  
497 not including the influence of the Fennoscandian ice sheet in this area. As noted above, we do not expect these

498 model runs to fully replicate the reconstructed characteristics of the BIIS (e.g. Clark et al., 2012). However, it is  
499 worth noting general, visually-derived, observations regarding the outputs shown in Figure 6. For larger  
500 temperature offsets, the ice sheet gets bigger, the timing of maximum extent gets progressively later and the  
501 modelled ice sheet gets thicker (Figure 6). In all experiments, there is generally a gradual advance toward the  
502 maximum extent followed by retreat (Figure 7). This pattern is interrupted by a later readvance that corresponds  
503 to the timing of the Younger Dryas in the GRIP record; this causes ice to regrow over high elevation areas such  
504 as Scotland and central Wales. The extent of this readvance increases with decreased temperature offsets between  
505 experiments (Figure 7). Smaller readvances, occurring around 16.5 ka also occur (Figure 7).

#### 506 **4.2 Geochronological data**

507 Ice-sheet advance dates were taken from the compilation of Hughes et al. (2016) and gridded to the ice sheet  
508 model domain (Figure 4). In total, 61 cells were represented with advance dates (Figure 8A). Considering now  
509 ice-sheet retreat (Figure 8B), dates deemed reliable or probably reliable by Small et al. (2017) were used (i.e.  
510 those given a ‘traffic light rating’ of green or amber). For the dated advance and retreat locations, the  
511 geochronological data in each cell was assigned an error corresponding to that which was reported in the literature.  
512 We also compared our results to the ‘likely’ empirical reconstruction of Hughes et al. (2016), based on that of  
513 Clark et al. (2012) (Figure 8C), using the minimum and maximum bounding envelopes to assign an error to each  
514 cell of the ice sheet grid (Figure 8D). The largest errors occur in the North Sea region, where there is a lack of  
515 empirical data (e.g. Figures 8A and B).

#### 516 **4.3 Results**

517 Table 4 shows selected statistics derived by ATAT when comparing the three ice-sheet modelling experiments  
518 (Figures 6 and 7) against the three categories of data (Advance, Retreat, Isochrones; Figure 8). wRMSE was not  
519 calculated for the DATED isochrone reconstruction, as grid points are distributed evenly and therefore have equal  
520 spatial weighting (Table 4). Experiment C produces modelled ice-sheets with the greatest areal extent, and  
521 therefore performs best at correctly covering the dated areas (Table 4). However, none of the three experiments  
522 perform particularly well when compared with the data or the empirical reconstruction regarding timing and  
523 results in high (>2000 year) RMSEs (Table 4). The application of ATAT and the results from these simplified  
524 experiments allow us to suggest directions for analysing future experiments.

525 All three experiments produced large RMSEs, in the order of thousands of years, when compared to all three  
526 categories of data (Table 4). For advance ages, the three simulations conform to a large number of dated locations  
527 (e.g. 72% of ages in Experiments B and C; Table 4). However, the RMSEs of advance ages are high (Table 4).  
528 This shows that, while the models perform well at matching the constraint of covering an area in ice after an  
529 advance age (Figure 3), the models often glaciates a region much later than required. Advance dates are particularly  
530 difficult to obtain from the stratigraphic record, and often there may be a long hiatus between the initial deposition  
531 of datable material and the subsequent advance of a glacier. Future experiments with large ensembles should  
532 therefore consider the number of advance dates conformed to (rather than the RMSE) as a more robust guide for  
533 model performance during ice advance.

534 For the retreat comparisons, the three modelling experiments conform to a larger percentage of sites, seemingly  
535 outperforming the empirically-derived DATED reconstruction (Table 4). However, where model-data agreement

536 occurs, the RMSE produced are much higher when ~~for~~ the model is compared to the DATED reconstruction. This  
537 is due to the reconstruction containing large uncertainties in regions which lack geochronological control (for  
538 example in the North Sea, Figure 8). These uncertainties, a product of spatial interpolation across regions with  
539 sparse information, are much greater than those associated with individual dates. Figure 9A shows examples of  
540 output maps from ATAT which display the spatial pattern of agreement and the magnitude of the difference  
541 between Experiment C and the DATED reconstruction. This shows that due to the uncertainty associated with  
542 North Sea glaciation, even where the model produces an unrealistic artefact, there is data-model agreement.  
543 Furthermore, ATAT produces a map which displays the number of years between data-based and modelled retreat  
544 and/or advance (e.g. Figure 9B). Figure 9B, which compares Experiment C to the DATED isochrones, shows that  
545 the timing of model-data disagreement is spatially variable. If more modelling simulations were conducted, such  
546 maps may reveal regions of reconstruction or particular dates which are difficult to simulate in the model. In such  
547 cases, data or model re-evaluation may be required and herein lies the potential utility of this ATAT tool in making  
548 sense of ensemble model runs. However, such model-data comparison awaits a full-ensemble simulation which  
549 accounts for model uncertainty (e.g. Hubbard et al., 2009).

## 550 5. Summary and concluding remarks

551 Here we present ATAT, an automated timing-accordance tool for comparing ice-sheet model output with  
552 geochronological data and empirical ice sheet reconstructions. We demonstrate the utility of ATAT through three  
553 simplified simulations of the former British-Irish Ice Sheet. Note that a ~~fuller~~-larger ensemble model of hundreds  
554 to thousands of runs is required for ~~full~~-model evaluation (e.g. Hubbard et al., 2009). ATAT enables users to  
555 quantify the difference between the simulated timing of ice sheet advance and retreat and those from a chosen  
556 dataset, and allows production of cumulative ice coverage agreement maps that should help distinguish between  
557 less and more promising runs. We envisage that this tool will be especially useful for ice-sheet modellers through  
558 justifying model choice from an ensemble, quantifying error and tuning ice-sheet model experiments to fit  
559 geochronological data. Ideally, this tool should be used in combination with other evaluation methods, such as fit  
560 to relative sea-level records. In the case where locations or regions of data cannot be fit by a model, and all model  
561 uncertainty has been accounted for in an ensemble simulation, the comparisons made in ATAT may also highlight  
562 that data re-evaluation is necessary. ATAT is supplied as supplementary material to this article.

## 563 6. Code Availability

564 ATAT 1.0-1 source code is freely distributed under a GNU GPL licence as supplementary material to this paper  
565 and can be downloaded from <https://figshare.com/s/38d0fd268684ad0fcc2d>. An example geochronological data  
566 grid can also be downloaded as supplementary material. The ice sheet modelling experiments shown here were  
567 conducted using the Parallel Ice Sheet Model (<http://pism-docs.org/>). Development of PISM is supported by  
568 NASA grant NNX17AG65G and NSF grants PLR-1603799 and PLR-1644277. The geochronological data used  
569 is freely available from <https://www.sciencedirect.com/science/article/pii/S0012825216304408#s0105> and  
570 <https://doi.pangaea.de/10.1594/PANGAEA.848117>.

571 **6.1. General Instructions**

572 ATAT is written in python, and distributed as both .py script, for use in Python 2, and a .py3 script, for use with  
573 Python 3. The tool requires installation of Python and the following freely available Python packages:

- 574 • netCDF4 (<https://pypi.python.org/pypi/netCDF4>)
- 575 • numpy (<http://www.numpy.org/>)
- 576 • scipy (<https://www.scipy.org/>)
- 577 • matplotlib (<https://matplotlib.org/>)
- 578 • matplotlib toolkit basemap (<https://matplotlib.org/basemap/>)

579 ATAT can be run from any Python enabled environment (e.g. IDLE, BASH). Here we provide the following  
580 simple instructions for running ATAT in a BASH shell. For numerous runs, a shell script should be created. Each  
581 stage has error reporting.

582 1. Open a BASH terminal and navigate to the directory containing the ATAT script (e.g. “cd /home/ATAT”).  
583 2. From the command line, launch the ATAT script using python (“python ATATv1.01.py”). Eight command-  
584 line arguments (A1 - A8), separated by a space should then follow.

585 A1: A command line prompt will ask whether dictates whether deglacial or advance ages are being tested. Type  
586 “DEGLACIAL” or “ADVANCE” accordingly, and press return.

587 4. A2 is the second prompt will ask for the path to the geochronological data file, type this in and press return (e.g.  
588 “/home/ATAT/geochron.nc”)

589 A3 defines the user whether the model extent is based on thickness or a mask. Type THK or MSK accordingly.

590 A4 5. is the The user is then asked to specify the path to the ice-sheet model output file (e.g.  
591 “/home/ATAT/icesheetmodel1.nc”)

592 6. A command line prompt will then ask the user whether the model extent is based on thickness or a mask. Type  
593 THK or MSK accordingly. In the case of MSK, the user is asked to define the numeric value of mask which  
594 represents grounded ice.

595 A5 is the value of the ice-sheet output mask. A value is required even if A3 = THK, but can be any value as it will  
596 be ignored.

597 A6 to A8 control output maps. A6 defines whether the output map should consider margin uncertainty, with a  
598 value of BORDER or NONE.

599 A7 defines whether the model-data offset map displaces RMSE (option “NONE”) or wRMSE (“WEIGHTED”).

600 A8 specifies which dates are plotted on the difference map, and can be “ALL” for all dates, “COVERED” for  
601 those which at some point where covered by ice and “INERROR” to display only those dates where model-data  
602 agreement within dating error occurred.

603 An example command would be “python ATATv1.1.py DEGLACIAL /home/ATAT/dated\_recon.nc MSK  
604 /home/ATAT/experiment1.nc 2 BORDER WEIGHTED INERROR”.

605 7.

606 ATAT then outputs the two maps and a csv table containing all derived statistics.

607 The user is then asked to define variables related to the output maps. For the model-data offset map (Figure 9B),  
608 either RMSE (type “NONE”) or wRMSE (type “WEIGHTED”) can be displayed for each site. For the cumulative

Formatted: Indent: First line: 0 cm

609 agreement map (Figure 9A), all sites (type “ALL”), those that the model glaciates at some point (type  
610 “COVERED”) or those that agree within error (type “INERROR”) can be displayed.  
611 8. ATAT then prints all statistics for the data model comparison conducted to a .csv file, default name  
612 “ATAT\_output.csv”.  
613

614 *Acknowledgements:* This work was supported by the Natural Environment Research Council consortium grant;  
615 BRITICE-CHRONO NE/J009768/1. [We thank Evan Gowan and Lev Tarasov for their constructive reviews which](#)  
616 [improved the manuscript.](#)

## 617 **References**

- 618 [Auriac, A., Whitehouse, P.L., Bentley, M.J., Patton, H., Lloyd, J.M. and Hubbard, A. Glacial isostatic adjustment](#)  
619 [associated with the Barents Sea ice sheet: a modelling inter-comparison. \*Quaternary Science Reviews\*, 147, 122-](#)  
620 [135, 2016.](#)
- 621 Applegate, P.J., Kirchner, N., Stone, E.J., Keller, K. and Greve, R. An assessment of key model parametric  
622 uncertainties in projections of Greenland Ice Sheet behavior. *Cryosphere*, 6(3), 589-606, 2012.
- 623 Arnold, J.R. and Libby, W.F. Radiocarbon dates. *Science*, 113(2927), 111-120, 1951.
- 624 Balco, G. Contributions and unrealized potential contributions of cosmogenic-nuclide exposure dating to glacier  
625 chronology, 1990–2010. *Quaternary Sci Rev*, 30(1), 3-27, 2011.
- 626 Bamber, J.L. and Aspinall, W.P.. An expert judgement assessment of future sea level rise from the ice sheets. *Nat*  
627 *Clim Change*, 3(4), 424-427, 2013.
- 628 Bateman, M.D., Evans, D.J., Roberts, D.H., Medialdea, A., Ely, J. and Clark, C.D., The timing and consequences  
629 of the blockage of the Humber Gap by the last British– Irish Ice Sheet. *Boreas*. 47(1), 41-61, 2018.
- 630 Boulton, G. and Hagdorn, M. Glaciology of the British Isles Ice Sheet during the last glacial cycle: form, flow,  
631 streams and lobes. *Quaternary Sci Rev*, 25(23), 3359-3390, 2006.
- 632 [Braconnot, P., Harrison, S.P., Kageyama, M., Bartlein, P.J., Masson-Delmotte, V., Abe-Ouchi, A., Otto-Bliesner,](#)  
633 [B. and Zhao, Y., 2012. Evaluation of climate models using palaeoclimatic data. \*Nature Climate Change\*, 2\(6\),](#)  
634 [417-424, 2012.](#)
- 635 Briggs, R.D. and Tarasov, L. How to evaluate model-derived deglaciation chronologies: a case study using  
636 Antarctica. *Quaternary Sci Rev*, 63, 109-127, 2013.
- 637 Briggs, R.D., Pollard, D. and Tarasov, L. A data-constrained large ensemble analysis of Antarctic evolution since  
638 the Eemian. *Quaternary Sci Rev*, 103, 91-115, 2014.
- 639 Brown, E.J., Rose, J., Coope, R.G. and Lowe, J.J. An MIS 3 age organic deposit from Balglass Burn, central  
640 Scotland: palaeoenvironmental significance and implications for the timing of the onset of the LGM ice sheet in  
641 the vicinity of the British Isles. *J Quaternary Sci*, 22(3), 295-308, 2007.
- 642 Bueler, E.D., Lingle, C.S. and Brown, J. Fast computation of a viscoelastic deformable Earth model for ice-sheet  
643 simulations. *Ann Glaciol*, 46(1), 97-105, 2007.
- 644 Bueler, E. and Brown, J. Shallow shelf approximation as a “sliding law” in a thermomechanically coupled ice  
645 sheet model. *J Geophys Res-Earth*, 114(F3), 2009.

646 Calov, R. and Greve, R. A semi-analytical solution for the positive degree-day model with stochastic temperature  
647 variations. *J Glaciol*, 51(172), 173-175, 2005.

648 Chiverrell, R.C., Thrasher, I.M., Thomas, G.S., Lang, A., Scourse, J.D., van Landeghem, K.J., Mccarroll, D.,  
649 Clark, C.D., Cofaigh, C.Ó., Evans, D.J. and Ballantyne, C.K. Bayesian modelling the retreat of the Irish Sea Ice  
650 Stream. *J Quaternary Sci*, 28(2), 200-209, 2013.

651 Clark, C.D., Hughes, A.L., Greenwood, S.L., Jordan, C. and Sejrup, H.P. Pattern and timing of retreat of the last  
652 British-Irish Ice Sheet. *Quaternary Sci Rev*, 44, 112-146, 2012.

653 Cornford, S.L., Martin, D.F., Graves, D.T., Ranken, D.F., Le Brocq, A.M., Gladstone, R.M., Payne, A.J., Ng,  
654 E.G. and Lipscomb, W.H. Adaptive mesh, finite volume modeling of marine ice sheets. *Journal of Computational  
655 Physics*, 232(1), 529-549, 2013.

656 DeConto, R.M. and Pollard, D. Contribution of Antarctica to past and future sea-level rise. *Nature*, 531(7596),  
657 591-597, 2016.

658 Duller, G.A.T. Single grain optical dating of glacial deposits. *Quaternary Geochronology*, 1(4), 296-304, 2006.

659 Dyke, A.S. An outline of North American deglaciation with emphasis on central and northern Canada.  
660 *Developments in Quaternary Sciences*, 2, 373-424, 2004.

661 Dyke, A.S. An outline of North American deglaciation with emphasis on central and northern Canada.  
662 *Developments in Quaternary Sciences*, 2, 373-424, 2004.

663 Edwards, T.L., Fettweis, X., Gagliardini, O., Gillet-Chaulet, F., Goelzer, H., Gregory, J.M., Hoffman, M.,  
664 Huybrechts, P., Payne, A.J., Perego, M. and Price, S. Effect of uncertainty in surface mass balance-elevation  
665 feedback on projections of the future sea level contribution of the Greenland ice sheet. *Cryosphere*, 8(1), 195-208.  
666 2014.

667 Fowler, A.C. A sliding law for glaciers of constant viscosity in the presence of subglacial cavitation. In  
668 *Proceedings of the Royal Society of London A: Mathematical, Physical and Engineering Sciences*, 407(1832),  
669 147-170, 1986.

670 Fretwell, P., Pritchard, H.D., Vaughan, D., Bamber, J.L., Barrand, N.E., Bell, R., Bianchi, C., Bingham, R.G.,  
671 Blankenship, D.D., Casassa, G. and Catania, G. Bedmap2: improved ice bed, surface and thickness datasets for  
672 Antarctica. *Cryosphere*, 7, 375-393, 2013.

673 Fuchs, M. and Owen, L.A. Luminescence dating of glacial and associated sediments: review, recommendations  
674 and future directions. *Boreas*, 37(4), 636-659, 2008.

675 Gasson, E., DeConto, R.M., Pollard, D. and Levy, R.H. Dynamic Antarctic ice sheet during the early to mid-  
676 Miocene. *Proceedings of the National Academy of Sciences*, 113(13), 3459-3464, 2016.

677 Golledge, N.R., Levy, R.H., McKay, R.M., Fogwill, C.J., White, D.A., Graham, A.G., Smith, J.A., Hillenbrand,  
678 C.D., Licht, K.J., Denton, G.H. and Ackert, R.P. Glaciology and geological signature of the Last Glacial  
679 Maximum Antarctic ice sheet. *Quaternary Sci Rev*, 78, 225-247, 2013.

680 Gomez, N., Pollard, D., Mitrovica, J.X., Huybers, P., Clark, P.U. Evolution of a coupled marine ice sheet-sea  
681 level model. *J Geophys Res*, 117, F01013, 2012.

682 Gomez, N., Pollard, D. and Mitrovica, J.X. A 3-D coupled ice sheet-sea level model applied to Antarctica through  
683 the last 40 ky. *Earth and Planet Sc Lett*, 384, 88-99, 2013.

684 Gowan, E.J. An assessment of the minimum timing of ice free conditions of the western Laurentide Ice Sheet.  
685 *Quaternary Sci Rev*, 75, 100-113, 2013.

686 Gregoire, L.J., Payne, A.J. and Valdes, P.J. Deglacial rapid sea level rises caused by ice-sheet saddle collapses.  
687 *Nature*, 487(7406), 219-222, 2012.

688 Greve, R. and Hutter, K. Polythermal three-dimensional modelling of the Greenland ice sheet with varied  
689 geothermal heat flux. *Ann Glaciol*, 21, 8-12, 1995.

690 Gudmundsson, G.H., Krug, J., Durand, G., Favier, L. and Gagliardini, O. The stability of grounding lines on  
691 retrograde slopes. *Cryosphere*, 6, 1497-1505, 2012.

692 Gudmundsson, G.H. Ice-shelf buttressing and the stability of marine ice sheets, *Cryosphere*, 7, 647-655, 2013.

693 Heroy, D.C. and Anderson, J.B. Radiocarbon constraints on Antarctic Peninsula ice sheet retreat following the  
694 Last Glacial Maximum (LGM). *Quaternary Sci Rev*, 26(25), 3286-3297, 2007.

695 Heyman, J., Stroeven, A.P., Harbor, J.M. and Caffee, M.W. Too young or too old: evaluating cosmogenic  
696 exposure dating based on an analysis of compiled boulder exposure ages. *Earth Planet Sc Lett*, 302(1), 71-80,  
697 2011.

698 Hindmarsh, R.C. Consistent generation of ice-streams via thermo-viscous instabilities modulated by membrane  
699 stresses. *Geophys Res Lett*, 36(6). 2009.

700 Hubbard, A., Bradwell, T., Gollidge, N., Hall, A., Patton, H., Sugden, D., Cooper, R. and Stoker, M. Dynamic  
701 cycles, ice streams and their impact on the extent, chronology and deglaciation of the British-Irish ice sheet.  
702 *Quaternary Sci Rev*, 28(7), 758-776, 2009.

703 Hughes, A.L., Greenwood, S.L. and Clark, C.D. Dating constraints on the last British-Irish Ice Sheet: a map and  
704 database. *J Maps*, 7(1), 156-184, 2011.

705 Hughes, A.L., Clark, C.D. and Jordan, C.J. Flow-pattern evolution of the last British Ice Sheet. *Quaternary Sci*  
706 *Rev*, 89, 148-168, 2014.

707 Hughes, A.L., Gyllencreutz, R., Lohne, Ø.S., Mangerud, J. and Svendsen, J.I. The last Eurasian ice sheets—a  
708 chronological database and time-slice reconstruction, DATED-1. *Boreas*, 45(1), 1-45, 2016.

709 Hughes, T.J., Is the West Antarctic ice sheet disintegrating? *J. Geophys. Res.*, 78 (33), 7884-7910, 1973.

710 Imbrie, J., Hays, J.D., Martinson, D.G., McIntyre, A., Mix, A.C., Morley, J.J., Pisias, N.G., Prell, W.L.,  
711 Shackleton, N.J. The orbital theory of Pleistocene climate: support from a revised chronology of the marine  $\delta^{18}O$   
712 record. In: Berger, A., Imbrie, J., Hays, H., Kukla, G., Saltzman, B. (Eds.), *Milankovitch and Climate, Part I*. D.  
713 Reidel Publishing, Dordrecht, 269–305, 1984.

714 Johnsen, S.J., Dahl-Jensen, D., Dansgaard, W. and Gundestrup, N. Greenland palaeotemperatures derived from  
715 GRIP bore hole temperature and ice core isotope profiles. *Tellus B*, 47(5), 624-629, 1995.

716 Kirchner, N., Hutter, K., Jakobsson, M. and Gyllencreutz, R. Capabilities and limitations of numerical ice sheet  
717 models: a discussion for Earth-scientists and modelers. *Quaternary Sci Rev*, 30(25), 3691-3704, 2011.

718 Kirchner, N., Ahlkrona, J., Gowan, E.J., Lötstedt, P., Lea, J.M., Noormets, R., von Sydow, L., Dowdeswell, J.A.  
719 and Benham, T. Shallow ice approximation, second order shallow ice approximation, and full Stokes models: A  
720 discussion of their roles in palaeo-ice sheet modelling and development. *Quaternary Sci Rev*, 147, 136-147, 2016.

721 Kleman, J., Hättestrand, C., Stroeven, A.P., Jansson, K.N., De Angelis, H. and Borgström, I. Reconstruction of  
722 Palaeo-Ice Sheets-Inversion of their Glacial Geomorphological Record. In Knight, P.G. (Eds) *Glacier science and*  
723 *environmental change*, 192-198, 2006.

724 Larour, E., Seroussi, H., Morlighem, M. and Rignot, E. Continental scale, high order, high spatial resolution, ice  
725 sheet modeling using the Ice Sheet System Model (ISSM). *J Geophys Res-Earth*, 117(F1), 2012.

726 Libby, W.F., Anderson, E.C. and Arnold, J.R. Age determination by radiocarbon content: world-wide assay of  
727 natural radiocarbon. *Science*, 109(2827), 227-228, 1949.

728 Lingle, C.S. and Clark, J.A. A numerical model of interactions between a marine ice sheet and the solid earth:  
729 Application to a West Antarctic ice stream. *J Geophys Res-Oceans*, 90(C1), 1100-1114, 1985.

730 Livingstone, S.J., Cofaigh, C.Ó., Stokes, C.R., Hillenbrand, C.D., Vieli, A. and Jamieson, S.S. Antarctic palaeo-  
731 ice streams. *Earth-Sci Rev*, 111(1), 90-128, 2012.

732 Lorenz, E.N. Deterministic Nonperiodic Flow, *J. Atmos. Sci.*, 20, 130-141, 1963.

733 Lowe, J.J. and Walker, M.J. Radiocarbon Dating the Last Glacial-Interglacial Transition (Ca. 14–9 14C Ka Bp)  
734 in Terrestrial and Marine Records: The Need for New Quality Assurance Protocols. *Radiocarbon*, 42(1), 53-68,  
735 2000.

736 Lowell, T.V., Fisher, T.G., Hajdas, I., Glover, K., Loope, H. and Henry, T. Radiocarbon deglaciation chronology  
737 of the Thunder Bay, Ontario area and implications for ice sheet retreat patterns. *Quaternary Sci Rev*, 28(17), 1597-  
738 1607, 2009.

739 Lukas, S., Spencer, J.Q., Robinson, R.A. and Benn, D.I. Problems associated with luminescence dating of Late  
740 Quaternary glacial sediments in the NW Scottish Highlands. *Quaternary Geochron*, 2(1), 243-248, 2007.

741 Mercer, J.H. West Antarctic ice sheet and CO<sub>2</sub> greenhouse effect: a threat of disaster. *Nature*, 271, 321-325, 1978.

742 Napijalski, J., Harbor, J. and Li, Y. Glacial geomorphology and geographic information systems. *Earth-Sci Rev*,  
743 85(1), 1-22, 2007.

744 Ó Cofaigh, C.Ó. and Evans, D.J. Radiocarbon constraints on the age of the maximum advance of the British–Irish  
745 Ice Sheet in the Celtic Sea. *Quaternary Sci Rev*, 26(9), 1197-1203, 2007.

746 Patton, H., Hubbard, A., Andreassen, K., Winsborrow, M. and Stroeven, A.P. The build-up, configuration, and  
747 dynamical sensitivity of the Eurasian ice-sheet complex to Late Weichselian climatic and oceanic forcing.  
748 *Quaternary Sci Rev*, 153, 97-121, 2016.

749 Pattyn, F. Sea-level response to melting of Antarctic ice shelves on multi-centennial timescales with the fast  
750 Elementary Thermomechanical Ice Sheet model (f. ETISH v1. 0). *Cryosphere*, 11(4), p.1851-1878, 2017.

751 Pattyn, F., Perichon, L., Aschwanden, A., Breuer, B., De Smedt, B., Gagliardini, O., Gudmundsson, G.H.,  
752 Hindmarsh, R., Hubbard, A., Johnson, J.V. and Kleiner, T. Benchmark experiments for higher-order and full  
753 Stokes ice sheet models (ISMIP-HOM). *Cryosphere*, 2(1), 111-151, 2008.

754 Pattyn, F., Schoof, C., Perichon, L., Hindmarsh, R.C.A., Bueler, E., Fleurian, B.D., Durand, G., Gagliardini, O.,  
755 Gladstone, R., Goldberg, D. and Gudmundsson, G.H. Results of the marine ice sheet model intercomparison  
756 project, MISMIP. *Cryosphere*, 6(3), 573-588, 2012.

757 Pollard, D. and DeConto, R.M. Modelling West Antarctic ice sheet growth and collapse through the past five  
758 million years. *Nature*, 458(7236), 329-332, 2009.

759 Ritz, C., Edwards, T.L., Durand, G., Payne, A.J., Peyaud, V. and Hindmarsh, R.C. Potential sea-level rise from  
760 Antarctic ice-sheet instability constrained by observations. *Nature*, 528(7580), 115-118, 2015.

761 Robinson, A., Calov, R. and Ganopolski, A. Greenland ice sheet model parameters constrained using simulations  
762 of the Eemian Interglacial. *Clim Past*, 7(2), 381-396, 2011.

763 Rutt, I.C., Hagdorn, M., Hulton, N.R.J. and Payne, A.J. The Glimmer community ice sheet model. *J Geophys*  
764 *Res-Earth*, 114(F2), 2009.

765 Schoof, C.S. Ice sheet grounding line dynamics: steady states, stability and hysteresis. *J. Geophys. Res. Earth*  
766 *Surf.*, 112, F03S28, 2007.

767 Schoof, C. Coulomb friction and other sliding laws in a higher-order glacier flow model. *Math Mod Meth Appl*  
768 *S*, 20(01), 157-189, 2010.

769 Schoof, C. Marine ice sheet stability. *J. Fluid Mech.*, 698, 62-72, 2012.

770 Seddik, H., Greve, R., Zwinger, T., Gillet-Chaulet, F. and Gagliardini, O. Simulations of the Greenland ice sheet  
771 100 years into the future with the full Stokes model Elmer/Ice. *J Glaciol*, 58(209), 427-440, 2012.

772 Seguinot, J., Rogozhina, I., Stroeven, A.P., Margold, M. and Kleman, J. Numerical simulations of the Cordilleran  
773 ice sheet through the last glacial cycle. *Cryosphere*, 10, 639-664, 2016.

774 Simpson, M.J., Milne, G.A., Huybrechts, P. and Long, A.J. Calibrating a glaciological model of the Greenland  
775 ice sheet from the Last Glacial Maximum to present-day using field observations of relative sea level and ice  
776 extent. *Quaternary Sci Rev*, 28(17), 1631-1657, 2009.

777 Small, D., Clark, C.D., Chiverrell, R.C., Smedley, R.K., Bateman, M.D., Duller, G.A., Ely, J.C., Fabel, D.,  
778 Medialdea, A. and Moreton, S.G. Devising quality assurance procedures for assessment of legacy  
779 geochronological data relating to deglaciation of the last British-Irish Ice Sheet. *Earth-Sci Rev*, 164, 232-250,  
780 2017.

781 Smedley, R.K., Glasser, N.F. and Duller, G.A.T. Luminescence dating of glacial advances at Lago Buenos Aires  
782 (~ 46° S), Patagonia. *Quaternary Sci Rev*, 134, 59-73, 2016.

783 Smedley, R.K., Chiverrell, R.C., Ballantyne, C.K., Burke, M.J., Clark, C.D., Duller, G.A.T., Fabel, D., McCarroll,  
784 D., Scourse, J.D., Small, D. and Thomas, G.S.P. Internal dynamics condition centennial-scale oscillations in  
785 marine-based ice-stream retreat. *Geology*, 45(9), 787-790, 2017.

786 Stokes, C.R., Tarasov, L., Blomdin, R., Cronin, T.M., Fisher, T.G., Gyllencreutz, R., Hättestrand, C., Heyman, J.,  
787 Hindmarsh, R.C., Hughes, A.L. and Jakobsson, M. On the reconstruction of palaeo-ice sheets: recent advances  
788 and future challenges. *Quaternary Sci Rev*, 125, 15-49, 2015.

789 Tarasov, L. and Peltier, W.R. A geophysically constrained large ensemble analysis of the deglacial history of the  
790 North American ice-sheet complex. *Quaternary Sci Rev*, 23(3), 359-388, 2004.

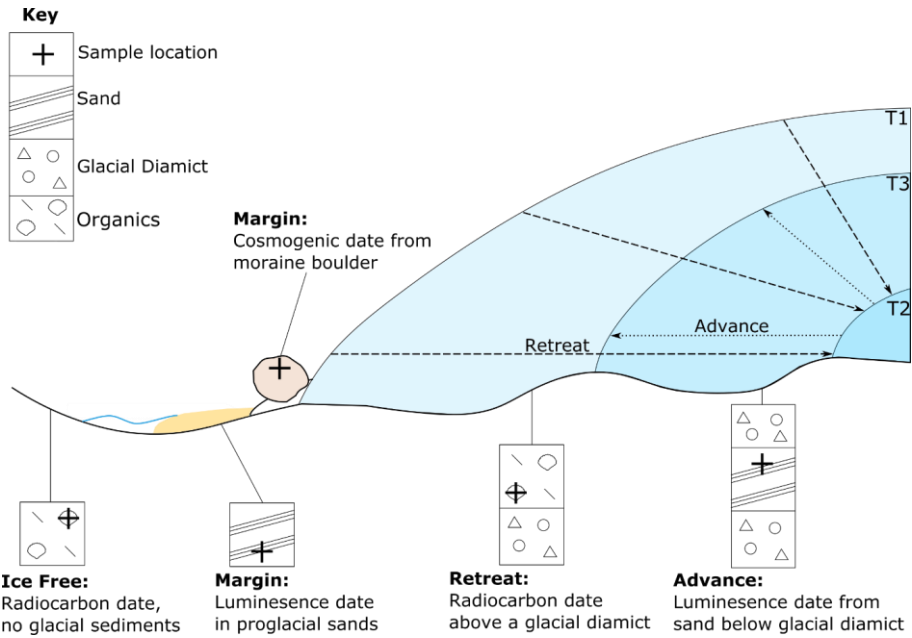
791 Tarasov, L., Dyke, A.S., Neal, R.M. and Peltier, W.R. A data-calibrated distribution of deglacial chronologies for  
792 the North American ice complex from glaciological modeling. *Earth Planet Sc Lett*, 315, 30-40, 2012.

793 Tushingham, A.M. and Peltier, W.R. Validation of the ICE-3G Model of Würm-Wisconsin Deglaciation using a  
794 global data base of relative sea level histories. *J Geophys Res-Solid Earth*, 97(B3), 3285-3304, 1992.

795 Weertman, J. Stability of the junction of an ice-sheet and an ice-shelf. *J. Glaciol*. 13 (67), 3-11, 1974.

796 Winkelmann, R., Martin, M.A., Haseloff, M., Albrecht, T., Bueler, E., Khroulev, C. and Levermann, A. The  
797 Potsdam parallel ice sheet model (PISM-PIK)-Part 1: Model description. *Cryosphere*, 5(3), 715-726, 2011.

798

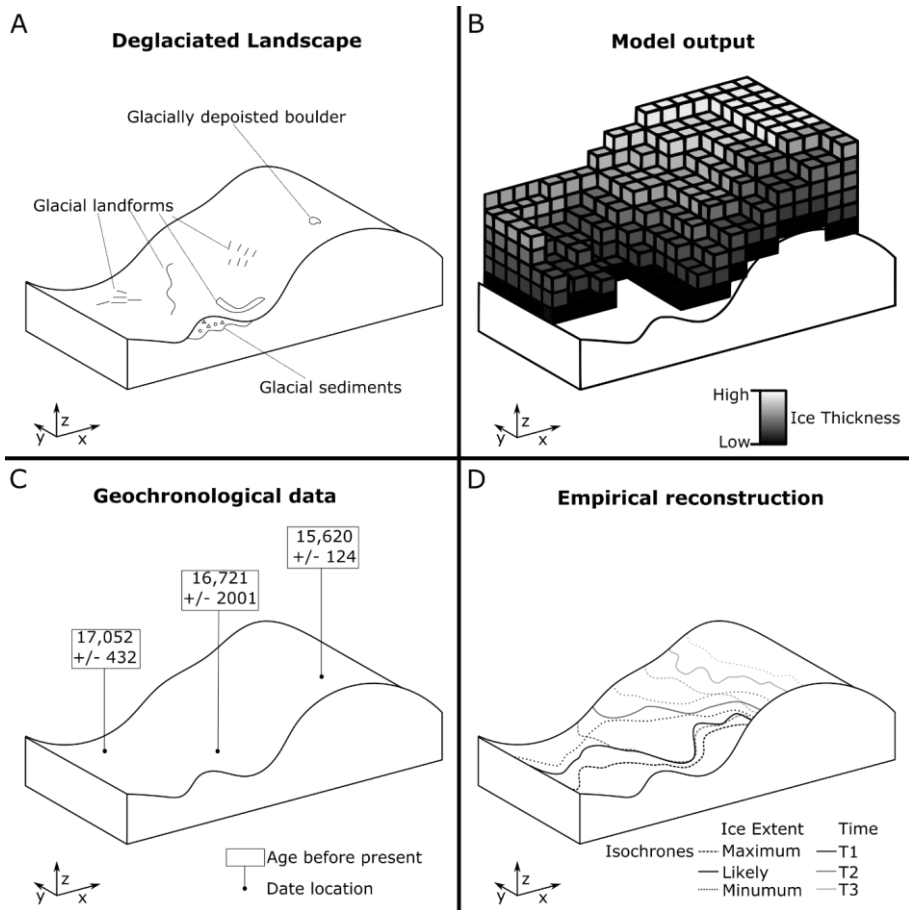


799

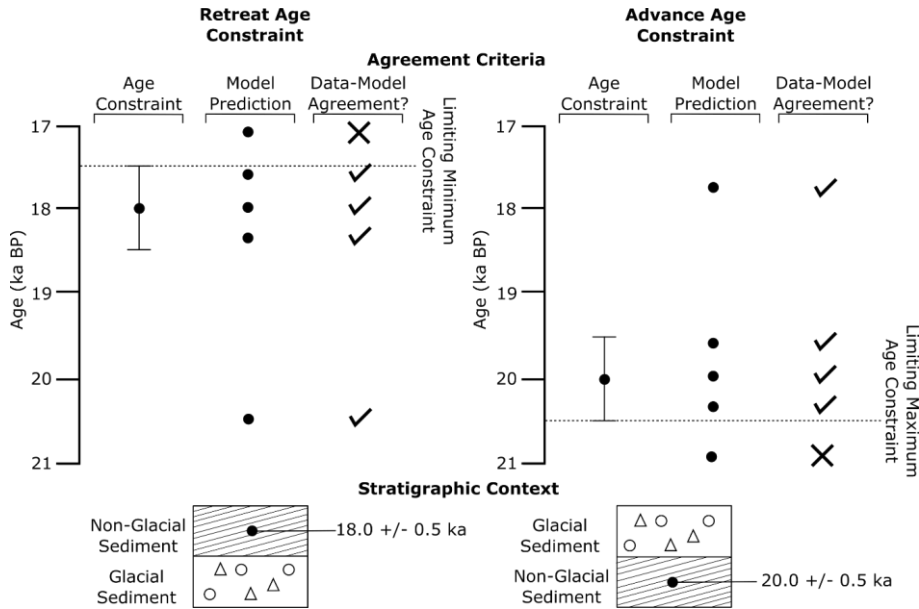
800

801

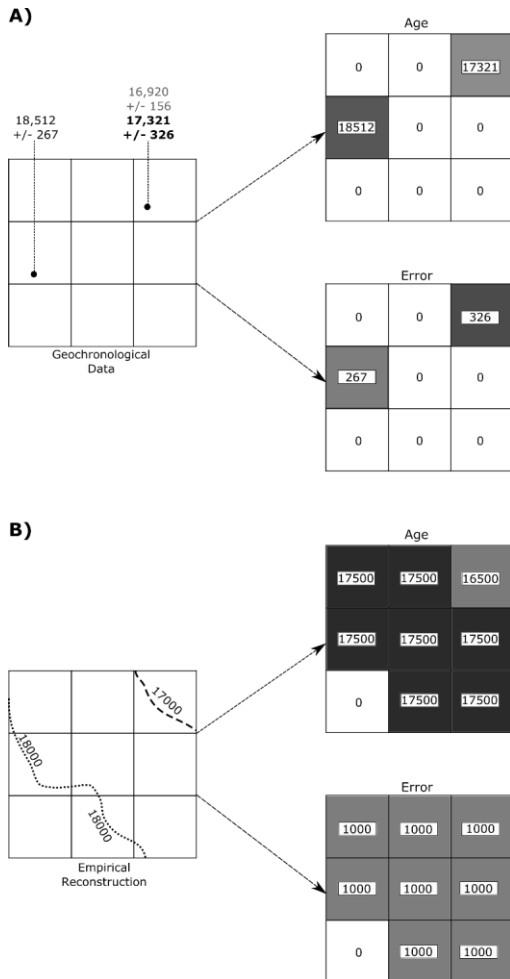
**Figure 1: Schematic illustration of stratigraphic and inferred glaciological context of geochronological data. Note that at T1 the ice sheet is at its most advanced. It then retreats to a minimum at T2, before re-advancing to T3.**



802  
 803 **Figure 2. Schematic of geochronological data and ice-sheet model output. A) A deglaciaded landscape,**  
 804 **demonstrating some of the features used by palaeo-glaciologists when empirically reconstructing an ice**  
 805 **sheet. B) Ice-sheet model output, displaying modelled ice-sheet thickness, in this case at a specific time. C)**  
 806 **Geochronological data. D) Empirical reconstruction. Note how the nature of these data vary between**  
 807 **source.**

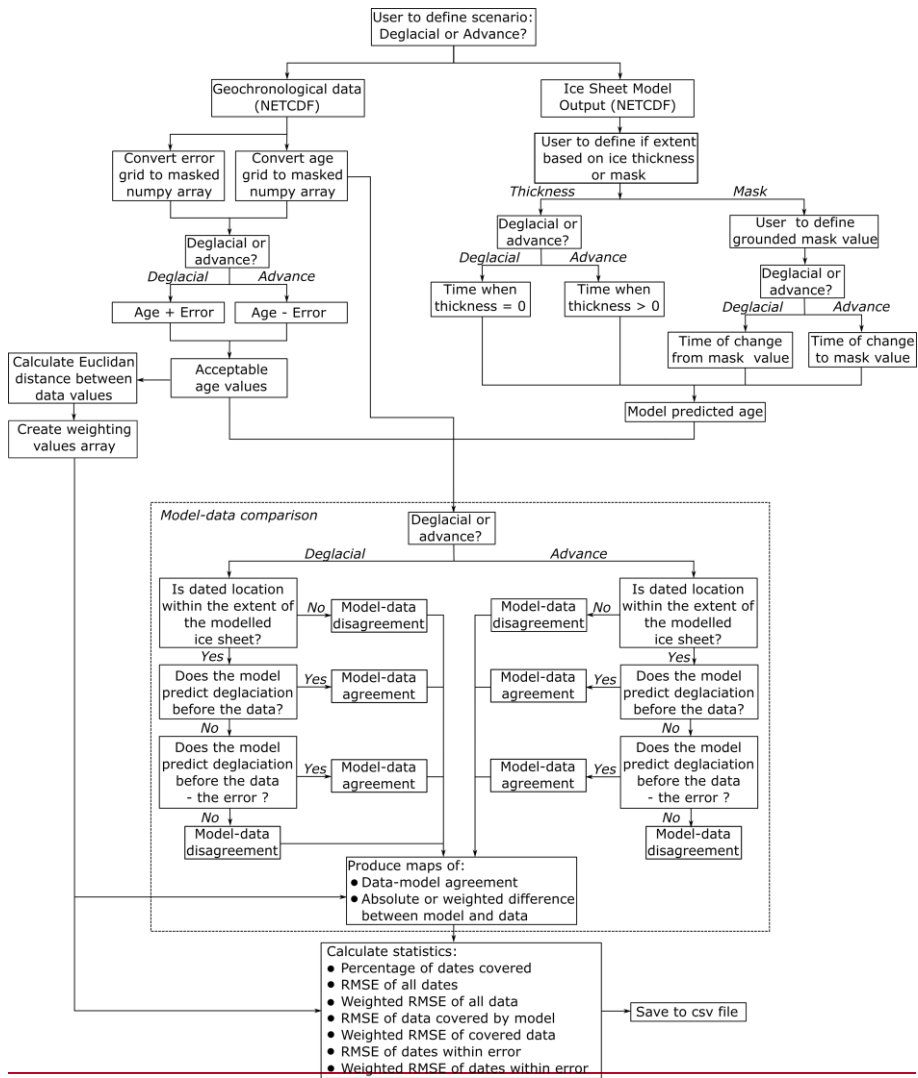


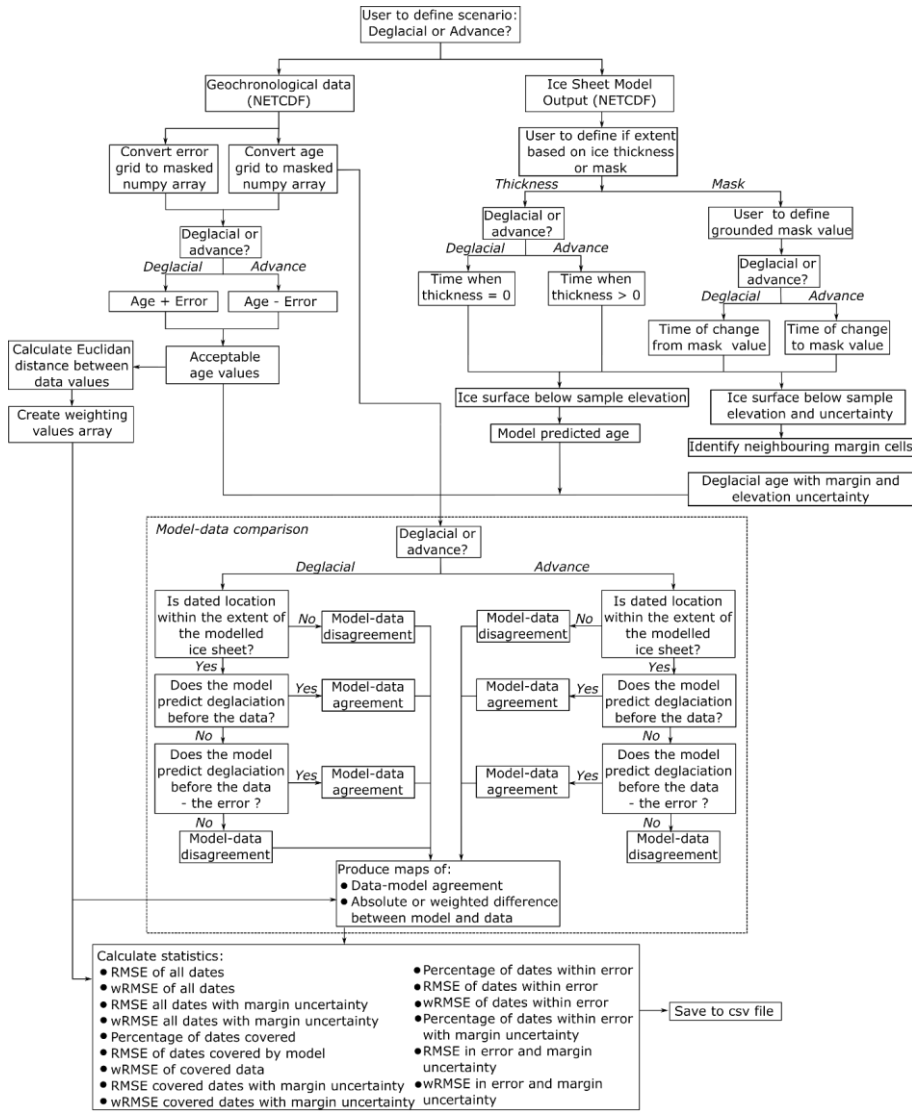
808  
 809 **Figure 3. Identification of data-model agreement with consideration of error by ATAT for retreat (left) and**  
 810 **advance (right) data. If a model predicts ice free conditions before an ice-free age, or during the associated**  
 811 **error, there is data-model agreement. If deglaciation occurs at this location after the error, the model**  
 812 **disagrees with the data. If a model predicts ice advance and cover before the advance age and its associated**  
 813 **error, there is model-data disagreement. Agreement between the model and data occurs if ice advances**  
 814 **over the location after the date, or before the date within the range of the error.**



815

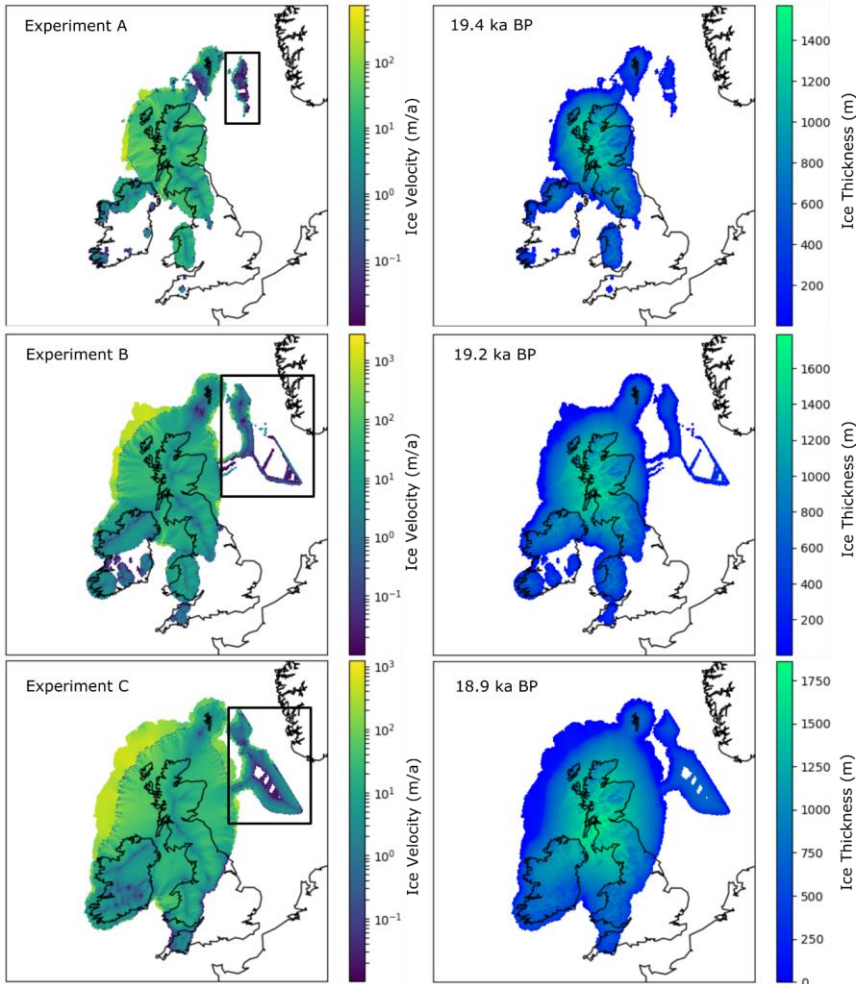
816 **Figure 4. Examples of empirical data preparation for ATAT. (A) Conversion of geochronological data into**  
 817 **a grid for ATAT. In this example the user has made a judgement based on a priori knowledge that the date**  
 818 **of 17,321 ± 326 is most representative of the event of interest. Note that age and error are split into separate**  
 819 **grids, and that no data regions are assigned a value of 0. (B) Conversion of an empirical reconstruction**  
 820 **(margin isochrones) into a grid for ATAT. Here we simply assume that the area between isochrones became**  
 821 **deglaciated between at the age between the two isochrones, and that associated error is 1000 years. More**  
 822 **complex reconstructions (e.g. Hughes et al., 2016) may require different user-defined rules.**



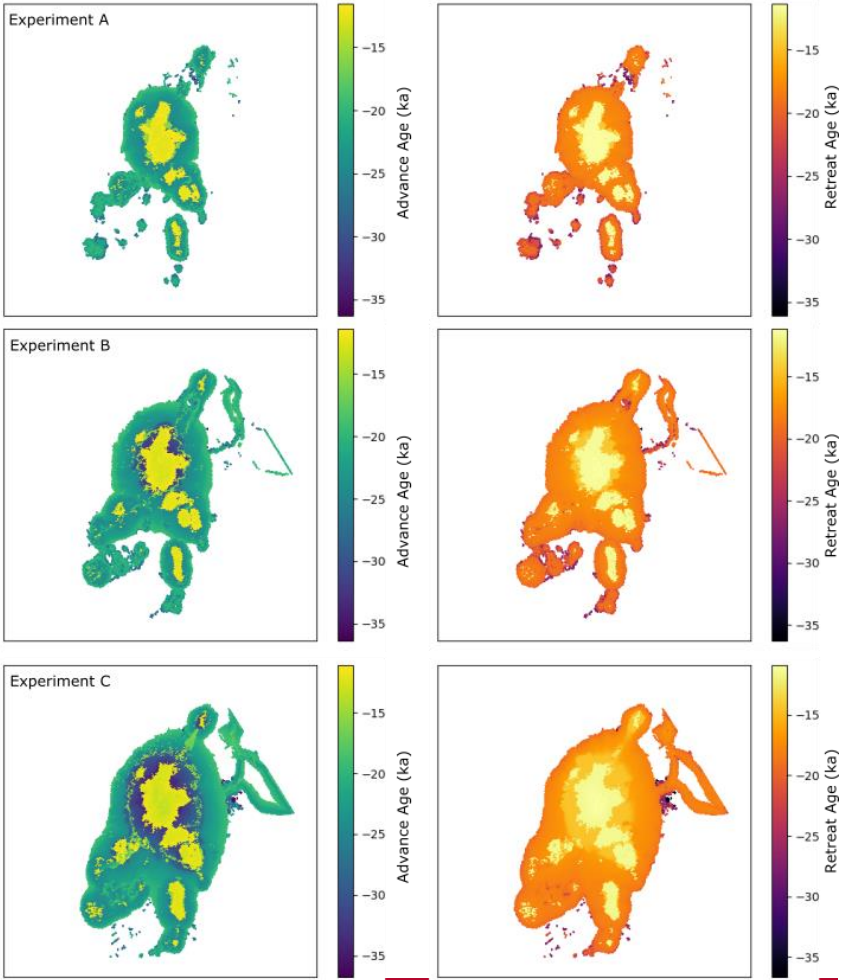


824

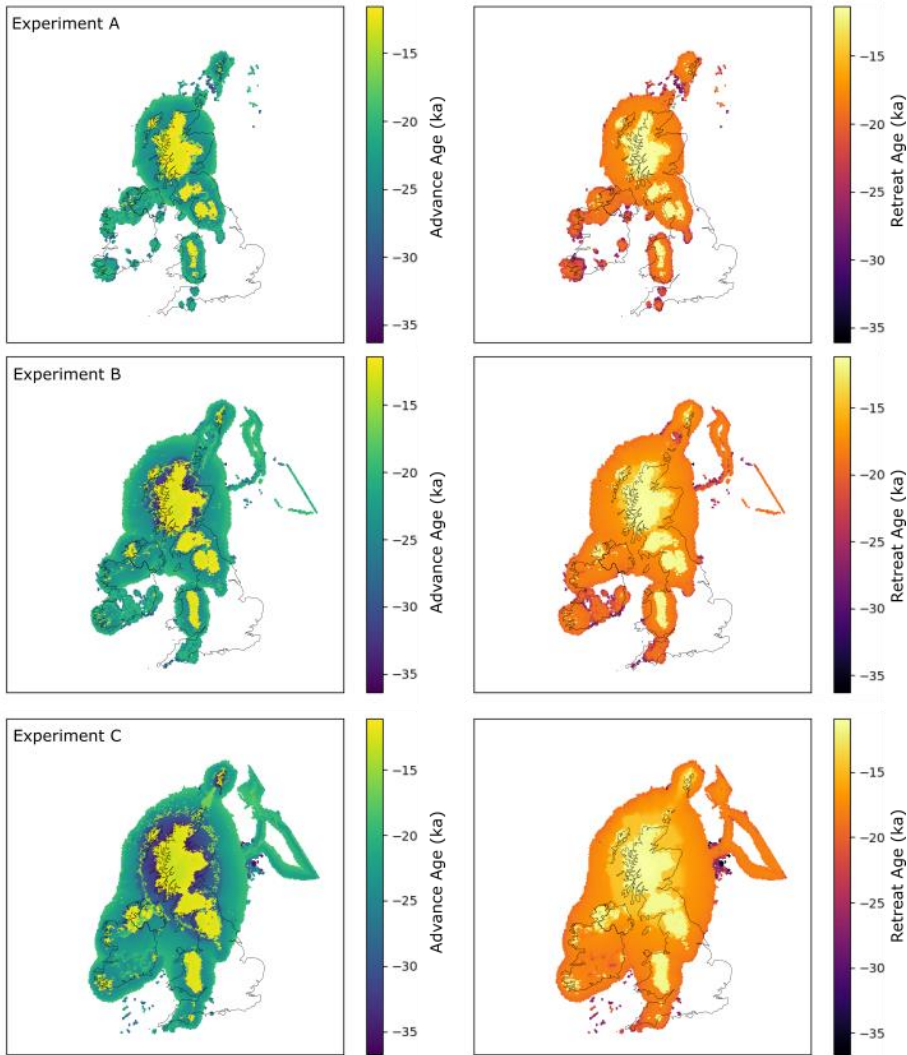
825 Figure 5. Flow chart of ATAT procedure. See text for further description.



826  
 827 **Figure 6. Maximum extent of produced ice sheet for the three experiments. Experiment B is 1°C colder**  
 828 **than A, and experiment C is 2°C colder than A. Left panel shows ice velocity, right is ice thickness. The box**  
 829 **on the left panel highlights likely erroneous output in the North Sea, likely a consequence of model domain,**  
 830 **discussed further in the text.**

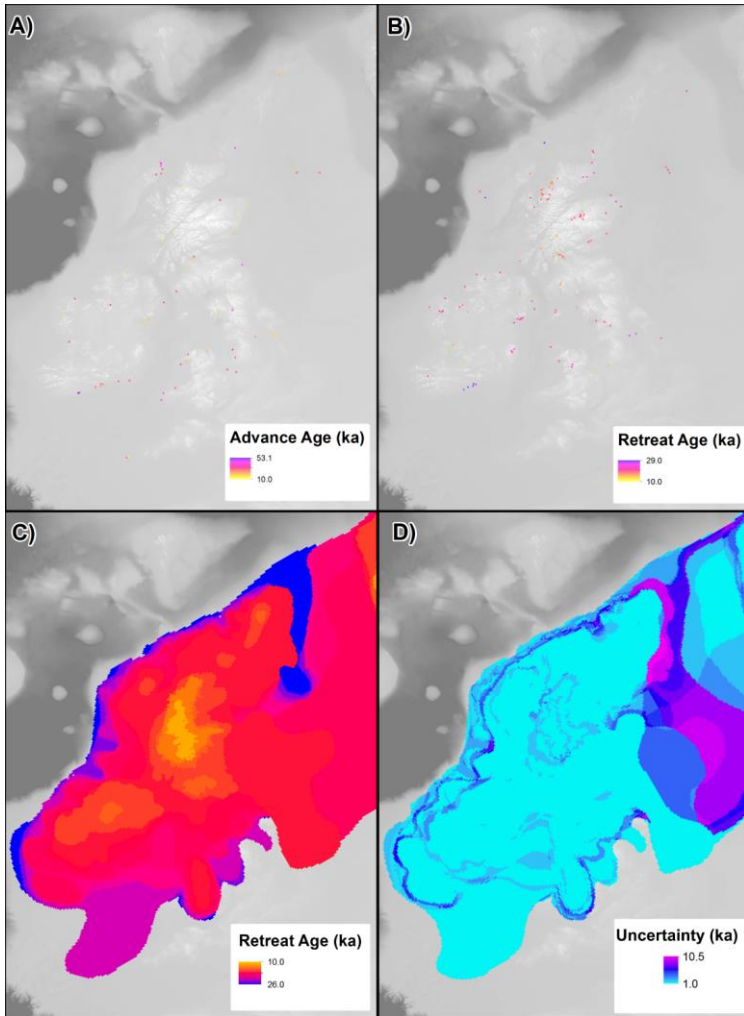


831

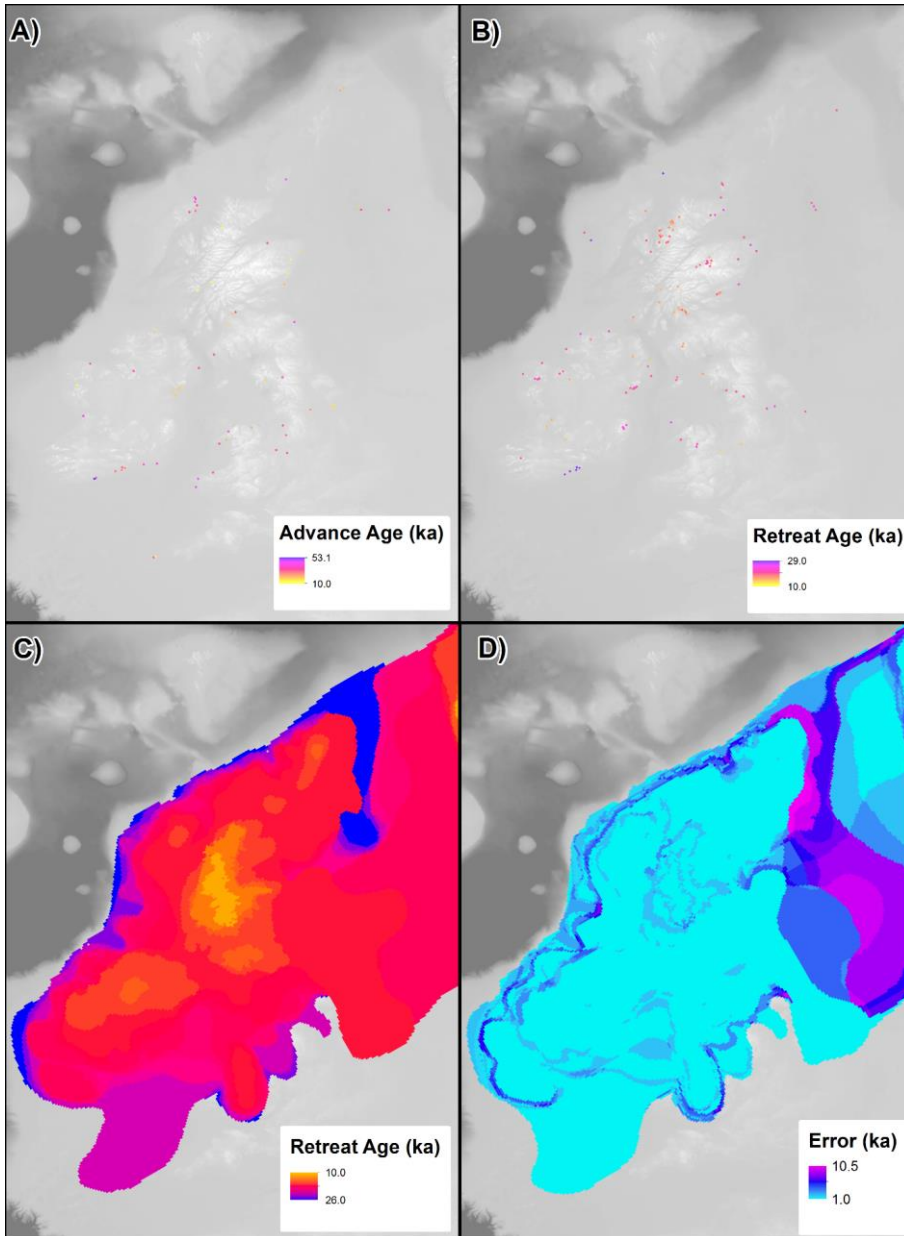


832

833 **Figure 7. Timing of advance (left) and retreat (right) from the three ice sheet modelling experiments.**  
 834 **Experiments are the same as in Figure 6. The early ages toward the centre of the model, and centred over**  
 835 **higher topography, represent the modelled extent of the Younger Dryas readvance.**

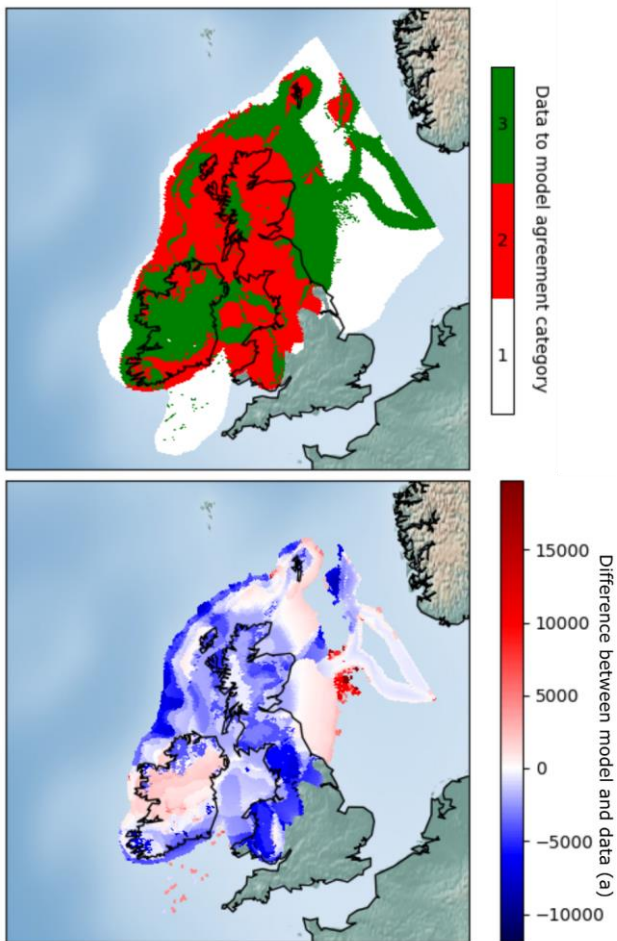


836



837

838 **Figure 8. Example of geochronological data projected onto model raster grids; as point-data in A and B**  
 839 **and from an empirical reconstruction in C and D. (A). Advance ages from Hughes et al. (2016). (B) Retreat**  
 840 **ages from Small et al. (2017). (C) Retreat age derived from DATED isochrone reconstruction (Hughes et**  
 841 **al., 2016). (D) Error associated with reconstruction in C.**



842  
 843 **Figure 9.** Example mapped outputs from ATAT. In this case, experiment C was compared with the DATED  
 844 reconstruction. Top map (cumulative agreement) shows categories of data-model agreement across the  
 845 domain, where 1 = not covered by model, 2 = no agreement and 3 = data-model agreement within error.  
 846 The lower map (model-data offset) shows magnitude of difference between model and data; negative values  
 847 show a modelled retreat of ice later than the DATED isochrones, and positive values show a modelled  
 848 retreat of ice before the DATED isochrones.

849 Table 1. Classification of geochronological data (after Hughes et al., 2011) and its use in ATAT.

<b>Class</b>	<b>Glaciological context</b>	<b>Stratigraphic context</b>	<b>Example</b>	<b>Use in ATAT</b>
Advance	Ice-sheet build up	Material directly below or incorporated within glacial diamict	Luminescence date from a sand below a glacial diamict	Ice cover a short time after this date
Retreat	Ice-free after ice cover	Dated material above glacial diamict	Radiocarbon date of a shell above a glacial diamict	Ice-free conditions from this date onwards (note deglaciation could have occurred a long time before)
Ice Free	Ice-free, but lacking direct information regarding ice	Dated material which indicates ice-free conditions but has no relation to ice cover. It may be much younger and not provide much useful constraint.	Radiocarbon date of organic sediments without underlying glacial sediments	
Margin	Proximal to an ice sheet margin	Dated material with information that ties it to an ice margin	Luminescence date in proglacial sands	
Exposure time (cumulative)	Length of time since sample exposed	N/A	Cosmogenic isotope on erratic boulder above a trimline	Not used

850

Table 2. Comparison of attributes between geochronological data and ice sheet model output.

	<b>Nature of data produced</b>	<b>Spatial resolution</b>	<b>Spatial continuity</b>	<b>Temporal frequency and resolution</b>	<b>Sources of uncertainty</b>	<b>Main limitation</b>
<b>Geochronological data</b>	Timing of the absence of ice at a location	Point location	Point location, unevenly distributed in space, but can be interpolated	Determined by data availability and associated error	Instrumental, environmental and stratigraphic factors	Reliant upon correct stratigraphic interpretation to tie to glaciological events
<b>Ice-sheet model output</b>	Simulation of physically plausible ice sheet conditions	Various, ranging from tens to unit kilometres.	Spatially even, regularly-spaced across entire domain	Continuous in time. Precise subannual resolution possible, but not recorded in practice	Parameterisations, boundary conditions	Based upon mathematical and physical approximations of ice flow

Data source	NetCDF Variable	Units	Dimensions	Description	Notes
	Time	<del>Years</del> before <u>presentTime</u> unit before reference calendar date	x, y	Calendar years before present	
Ice sheet model output	thk	m	time, x,y	Ice thickness	Either “thk” or “msk” required by ATAT.
	msk	Integers	time, x,y	Grounded/floating/icefree mask	Either “thk” or “msk” required by ATAT. User defines value referring to the location of grounded ice
	lat	Decimal degrees	x, y	Latitude	
Both	lon	Decimal degrees	x, y	Longitude	
	age	<u>Time unit</u> before reference calendar date <del>Years</del> before present	x, y	Timing of deglaciated conditions	Deglacial and advance ages must be in separate files.
Geochronological data	error	<del>Years</del> <u>Seconds</u> ds	x, y	Error associated with deglaciated conditions	Error associated with either deglacial and advance age

must be in associated separate  
file.

<u>topg</u>	<u>m</u>	<u>x,y</u>	<u>Modern elevation at resolution of ice-sheet model</u>
<u>elevation</u>	<u>m</u>	<u>x,y</u>	<u>Elevation of collected sample</u>

Table 3. Required input variables for ATAT NetCDF files.

Table 4: Example statistics from ATAT. Note that the RMSE is often altered by applying the spatial weighting to create wRMSE.

	<u>Advance</u>			<u>Retreat</u>			<u>Empirical Reconstruction: DATED</u>		
<u>Ice Sheet Modelling Experiment</u>	<u>A</u>	<u>B</u>	<u>C</u>	<u>A</u>	<u>B</u>	<u>C</u>	<u>A</u>	<u>B</u>	<u>C</u>
<u>Percentage of dates covered</u>	<u>52.5</u>	<u>72.1</u>	<u>88.5</u>	<u>76.1</u>	<u>91.7</u>	<u>96.3</u>	<u>32.9</u>	<u>52.6</u>	<u>69.8</u>
<u>Percentage that agree within error</u>	<u>65.6</u>	<u>72.7</u>	<u>72.2</u>	<u>22.0</u>	<u>22.0</u>	<u>12.8</u>	<u>23.2</u>	<u>27.0</u>	<u>17.8</u>
<u>RMSE dates covered by model</u>	<u>11075.9</u>	<u>12732.7</u>	<u>13490.3</u>	<u>3879.0</u>	<u>4180.9</u>	<u>4945.4</u>	<u>2972.5</u>	<u>2678.0</u>	<u>2920.8</u>
<u>wRMSE dates covered by model</u>	<u>13357.3</u>	<u>13994.7</u>	<u>14849.7</u>	<u>4073.4</u>	<u>4450.3</u>	<u>5165.8</u>	<u>N/A</u>	<u>N/A</u>	<u>N/A</u>
<u>RMSE dates within error</u>	<u>655.7</u>	<u>478.6</u>	<u>289.3</u>	<u>403.6</u>	<u>259.7</u>	<u>236.2</u>	<u>12023.4</u>	<u>10638.7</u>	<u>8777.6</u>

<u>wRMSE</u>	<u>615.4</u>	<u>395.0</u>	<u>223.6</u>	<u>422.1</u>	<u>276.9</u>	<u>248.9</u>	<u>N/A</u>	<u>N/A</u>	<u>N/A</u>
<u>dates within</u>									
<u>error</u>									